Methods of Measuring Stress Relaxation in Composite Tape Springs

THESIS

Justin T. Heppe, Capt, USAF

AFIT-ENY-MS-15-M-221

DEPARTMENT OF THE AIR FORCE
AIR UNIVERSITY

AIR FORCE INSTITUTE OF TECHNOLOGY

Wright-Patterson Air Force Base, Ohio

AFIT-ENY-MS-15-M-221

METHODS OF MEASURING STRESS RELAXATION IN COMPOSITE TAPE SPRINGS

THESIS

Presented to the Faculty

Department of Aeronautics and Astronautics

Graduate School of Engineering and Management

Air Force Institute of Technology

Air University

Air Education and Training Command

in Partial Fulfillment of the Requirements for the

Degree of Master of Science in Aeronautical Engineering

Justin T. Heppe, B.S. Aerospace Engineering

Capt, USAF

March 26, 2015

AFIT-ENY-MS-15-M-221

METHODS OF MEASURING STRESS RELAXATION IN COMPOSITE TAPE SPRINGS

THESIS

Justin T. Heppe, B.S. Aerospace Engineering
Capt, USAF

Committee Membership:

Dr. A. Jennings
Chair

Dr. E. Swenson
Member

Mr. W. Reynolds
Member

Abstract

Composite tape springs present an opportunity to use stored energy for the deployment of space structures. Concern has risen over the dissipation of strain energy during storage due to viscoelasticity inherent in polymeric materials commonly used as the composite matrix. Tests to measure the internal behavior of a composite tape spring over time are conducted along with methods of analyzing and fitting the resulting data. The three constant strain configurations tested were compression force of the cross section, a restraining force of a longitudinal fold, and the change in shape of a folded section. While the shape changing test did not appear to be sensitive enough, the stress tests proved useful for measuring relaxation.

Table of Contents

Page

List of Figures

List of Tables

METHODS OF MEASURING STRESS RELAXATION IN COMPOSITE TAPE SPRINGS

I. An Introduction to Tape Springs

A tape spring is a structure of semi-elliptical cross section, with length much greater than width and width much greater than thickness. Extended and folded tape springs are shown in Figure 1. A tape spring can be rolled around itself compressing its semi-elliptical shape flat which provides the "spring" properties. The most familiar form of tape spring is found as the tape in carpenter tape measures, commonly made of steel. The unique shape of the tape allows rolling and storage in a small space, provides a deployment force due to its spring properties, while also being semi-rigid when unrolled to make measurements easier. A tape spring for the purpose of this thesis will be made of a quartz fiber/epoxy resin matrix composite with a $\pm 45/0/\pm 45$ layup. The tape spring is cured in a semi-elliptical shape of greater curvature than a tape measure, providing greater deployment force and a more rigid deployed form.

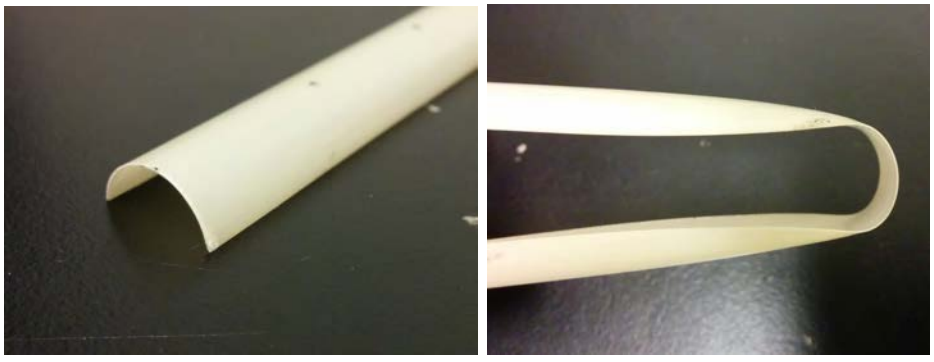

Figure 1. Tape Spring Extended and Folded

Tape springs as deployable space structures offer many advantages that make them desirable for future satellite and space vehicle design. The launch expense of

a space vehicle is directly related to its weight and size. Tape springs can be rolled or otherwise placed in compact storage during launch that can then deploy to create large structures in space. Non-deployable designs are constrained to the size of the launch vehicle bay. Other deployable structures may rely on independent means for deployment force. These additional deployment means are unnecessary for anything other than the deployment and thus are dead weight for a majority of the mission. Removing this weight and placing the deployment means within the structure itself eliminates this excess. Tape springs are also scalable in size and may present new designs for large space structures. The ability to deploy large structures presents further possibilities for new and improved functionality of space vehicles. This chapter provides a review of the problem, background, and assumptions of concern in this thesis.

1.1 Background

Rolled storage and deployment of tape springs, while offering the benefits mentioned above, also presents a new set of challenges in fully understanding the behavior. The Air Force Research Laboratory Space Vehicles Directorate (AFRL/RVSV) outlined one of these challenges as understanding the affect of long term storage in the rolled configuration on the deployment behavior. If this effect of storage is significant, can potential methods be developed to prevent these effects? AFRL's questions are important to space vehicle design for a number of reasons. Most of these vehicles are built, tested, and then stored for months to years while they await launch. If the tape springs degrade during storage, deployment may be negatively affected to the point of failure. The failure of a space vehicle to deploy properly may make the spacecraft non-functional and force an entirely new spacecraft to be built and launched with the associated costs. Numerous reports have been published discussing the means,

mechanisms and effects that are inherent when using polymer matrix composites. AFRL/RVSV and AFIT have also performed a number of internal tests to better understand the composite tape spring. What is not available currently is a consistent means to test the long term behavior of a rolled tape spring as near directly as possible. This thesis is the first attempt at AFIT to test this behavior in a tape spring.

1.2 Problem Statement

This thesis will explore a means to test the long term behavior of a rolled tape spring. The problem statement: *Is there a means of measuring the internal behavior of a tape spring in its rolled configuration?* The purpose of this problem is to better understand the viscoelastic response of the tape spring in rolled storage. To achieve this, several questions are formulated, the successful answering of which will provide sufficient evidence that a viable test setup has been found. Deployment of a tape spring will be primarily affected by the internal stress energy available that attempts to return the object to its extended shape. Change in internal stress is historically measured through creep or stress relaxation tests. Since a rolled tape spring is at a constant strain it should experience stress relaxation and this is the desired property to measure. The first question: *Are there methods of imitating the rolled configuration in which changes in internal stress can be measured via stress relaxation?* The fact that tape springs show stress relaxation in storage configuration has been shown [1, 12, 13, 17]. If no stress relaxation is shown in the tests than the behavior of interest is not being captured. If stress relaxation is measured, the next question is: *Is the behavior consistent and reasonable?* If the behavior is both consistent and reasonable, the test can be credited as measuring a valid behavior and a model can be created for predicting the future behavior of a rolled tape spring.

The final two questions are outside the main scope of this thesis but important to consider. Temperature is typically heavily linked to dynamic behaviors and thus internal strain and stress of the material. When performing tests, temperature also affects the measuring devices. The third question is: *What is the effect of temperature?* Determining the effect of temperature will allow the modeling of a tape spring subjected to a temperature profile during storage. Another question of great interest is: *What is the effect of allowing the tape spring to return to its extended form after a period of deformation?* This question attempts to increase our understanding of tape springs and answer if this may be a means of preventing some negative effects of rolled storage.

To address all four questions a thorough investigation of the current theory and research into tape springs and composite aging is performed. Next to address the first two questions solely, using current theories, a number of tests are designed and performed. Further details of the methods to be used are given in Chapter III.

1.3 Scope of Analysis

The problem statement and associated tests intend to provide a means of repeatably measuring the changes in internal stress encountered in a rolled tape spring. By characterizing this behavior, the internal stress available at any point in the life of the rolled tape spring can be predicted using extrapolation and modeling of the measured data. This approximate internal stress can be correlated to the deployment behavior by simple relational tests. Thus the internal stress provides a means for determining the affect of long term storage in the rolled configuration on deployment behavior. What will not be determined from these tests are the affects on deployment caused by means other than changes in internal stress, such as chemical or mechanical deterioration. Affects on deployment by internal stress levels are expected to account for

a large portion of the behavior of interest; however, other affects may not be trivial. Also, the actual changes in deployment behavior related to the measured changes in internal stress will not be correlated through these tests.

1.4 Assumptions

Many possible causes of the changes in internal stress are dependent on the surrounding environment and history of the material. Therefore, the following assumptions are made. The first assumption is that manufacturing and storage variances are minimal. Tests will be performed with various test articles obtained from different production lots. The forty-one tests to be performed can allow a determination only of the validity of the manufacturing variances assumption. The tests will not be able to pinpoint how manufacturing variances affect stress relaxation. The second assumption is that the laboratory environment closely resembles the storage conditions that will be seen by an actual stored space vehicle. The fluctuations in the test environment will add scatter to the results; however, it is assumed this scatter will be the same seen in actual storage of a tape spring on a space vehicle. Due to the introductory nature of this thesis, investigation of the important area of dynamic behavior must be overlooked. An initial deployment test was performed; however, correlation of the stress relaxation with changes in deployment is outside of scope of this thesis. The assumption will be made that a lower internal stress will lead to reduced deployment speeds with the magnitude of this correlation remaining unknown.

1.5 Summary

The benefits of tape springs in space vehicle design are numerous but they introduce technical challenges that must be understood and solved in order to create a robust design. The problem of interest to this thesis is discovering a means of mea-

suring the internal behavior of the tape spring in its rolled configuration. Subsequent chapters will discuss the current theory and experimental data in Chapter II, the method used to collect and analyze necessary data in Chapter III, the results of these data and analysis in Chapter IV, and the conclusions to the questions outlined in Chaper V.

II. Current Tape Spring Theory and Experimental Data

The purpose of Chapter II is to review current theory and experimental data available in literature to gain perspective on the problem to be addressed and a path forward to solution. The chapter will start with a review of specific issues with the tape spring life cycle between fabrication and deployment in Section 2.1. The discussion will include the issues unique to space usage. The chapter will continue with a review of composites in general to include its raw materials, fabrication, inspection, and assembly in Section 2.2. Discussion of the theory behind time dependent properties of all materials including aging, creep and stress relaxation will follow in Section 2.3. A review of standards of note, and studies performed investigating the time dependent effects in composites and tape springs will be presented in Sections 2.4 and 2.5. Finally, conclusions from the information will be reviewed as well as expectations for the problem of interest in this thesis.

2.1 Expected Conditions and Properties Required

The tape spring is subjected to varying environments throughout its life cycle. Initially, the fiber is pre-impregnated with the resin (or matrix) material, and is now referred to as a pre-preg. The pre-preg is frozen at -18°C and transported to the fabricator of the tape spring. Once delivered to the fabricator the pre-preg will remain refrigerated until fabrication where it is warmed to room temperature, cut to size, collated (lay-up), and pressed on a tool to final shape. On the tool, the tape spring is placed in a vacuum bag and heated through the curing cycle specified by the pre-preg manufacturer [3].

After curing, the part is removed from the tool and shipped to the space vehicle assembly facility. At the assembly facility, the tape spring is attached to the space

vehicle. As an assembly, the tape spring may be tested by being rolling into its storage shape and then deployed. After successful deployment, the tape spring is rolled again into its storage shape and remains rolled until deployment in orbit. The space vehicle is placed into storage after assembly is complete. Storage may last from months to years depending on launch priority and opportunity. Once the space vehicle is selected for launch, it is removed from storage, tested for operation, and placed in the payload bay of the launch vehicle. The launch vehicle is further assembled and placed onto its launch pad. The launch vehicle may remain on its pad for days to weeks depending on weather and mechanical difficulties. Typically, payload bays are not temperature controlled and launch sites are commonly located in tropical climates. During launch the space vehicle is subjected to rapid acceleration and temperature changes. Once the space vehicle is released from the payload bay, it is now in the space environment. Assuming the space vehicle is in low earth orbit (LEO) it travels in and out of the earths shadow causing frequent cycles of temperature extremes. In LEO there is no atmospheric reduction of radiation so the space vehicle is subject to bursts of high level radiation. Also, in LEO the amount of atomic oxygen present can be sufficient to significantly degrade many organic materials including those used as matrix material in composite tape springs [5].

It is in space that the tape spring is deployed to its final extended shape. The effect of this storage and temperature history on the tape spring must be understood and modeled in order for the space vehicle manufacturer and operator to be sure the tape spring will deploy in the manner designed. Further consideration of the tape spring composition and fabrication will be discussed below providing detail to begin understanding this time history.

2.2 Composites Review

It is necessary to understand how a composite tape spring is actually created in order to understand its properties. This understanding includes why the specific fiber, matrix material, and ply orientations are chosen. How the tape spring is tooled and cured significantly influences the expected quality. How close the final material properties are to the design is a function of the quality of manufacturing. Potential methods to commercialize the process and how assembly occurs is also reviewed. This early life history will give a better understanding of potential reasons for experimental variances as well as potential methods to prevent issues encountered.

Fiber.

For a tape spring used in the space environment, an ideal fiber will provide the required strength but also maintain consistent properties through the drastic temperature cycles over a long period of time. Different fiber materials can also provide various electric and thermal properties to the composite part. For example, layers can be inserted to add antenna functionality [2]. For this tape spring the assumption is made that it is purely intended for structural purposes and will require no thermal or electric considerations. Fibers can be made of many different materials; however, there are three major families of fiber types used in structural applications: glass, carbon, and aramid (or organic). Glass fibers include E-glass, S-2 Glass, and quartz. Carbon fibers include pitch and pan based types. One of the most recognized form of aramid fiber includes Kevlar®. Glass fibers are typically the least expensive with aramid and carbon fibers increasing in price respectively.

Figure 2 shows various material properties for these high strength fiber types, the dot size represents the elongation at failure percentage [3]. From these properties it can be seen that the E-Glass and S-2 Glass fibers, which are less expensive, have

relatively high coefficients of thermal expansion compared to the more expensive quartz. Composite degradation can occur through fiber matrix separation. A higher coefficient of thermal expansion leads to fewer temperature cycles before degradation occurs. Quartz elongation at failure, while low compared to its glass counterparts, is much higher than carbon fiber and quartz has a much lower tensile modulus. These properties mean that a quartz composite can stretch further without failing [3]. The low coefficient of thermal expansion and the high elongation at failure are properties ideal for tape springs. Using Murphey's concentrated strain metric ($E * \varepsilon^2$) also shows the importance of the high elongation at failure in increasing available strain of the material [18]. Another concern is the fiber conductivity, which for carbon fibers complicate the antenna design due to its conductive nature. Glass fibers are insulators and thus do not present additional complexity in antenna design. Therefore, quartz provides an ideal fiber material for use in tape springs.

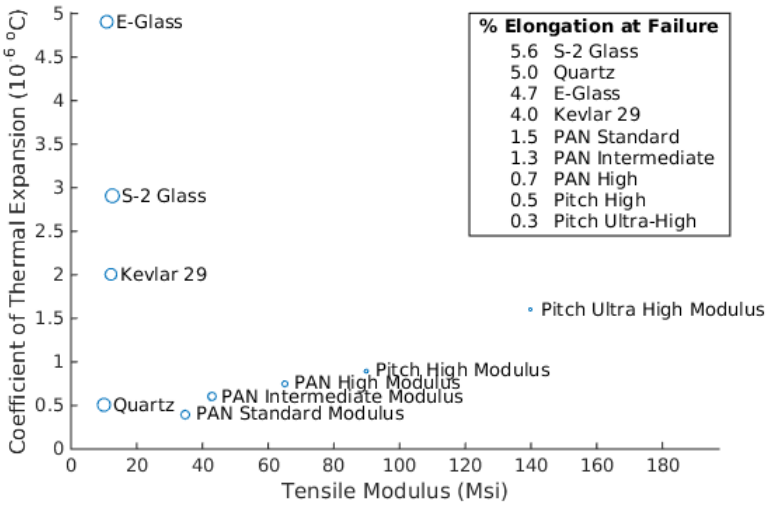

Figure 2. Various High Strength Fiber Properties

Matrix or Resin.

A composite tape spring used in the space environment requires a matrix that can also handle the large variations in temperature experienced on orbit while maintaining good durability. If used in LEO, the matrix must be resistant to atomic oxygen or coated to protect from this corrosive agent [5]. The matrix also has to resist outgassing, or the loss of internal contaminates, in the vacuum of space. This outgassing can cause deformations in shape that are undesirable for antenna, optics or other structures sensitive to material dimensions.

Similar to the fibers, a matrix can be constructed using nearly any type of material. Common advanced composites use polymers, metals, or ceramics. For tape springs the ideal material is a polymer. Polymers are broken into two major classes: thermosets and thermoplastics. Thermosets chemically bond together when cured to create a cross-linked structure. This cross-link cannot be undone without destroying the molecules themselves, thus thermosets are permanent. Thermoplastics do not cross-link and are able to be heated and reformed into different shapes. Thermoplastics require high temperatures to melt (260-425°C), and once melted are highly viscous making mating with the fibers difficult. Mating difficulty makes thermoplastic pre-preg materials difficult to manufacture and expensive. Thermoplastic pre-pregs are also solid by nature since the polymer is in its final form and requires no curing. Since the thermoplastic is solid it cannot be layed up like thermosets but must be fused together through more complicated means at or near its melting temperature. Once fused the thermoplastic component must be heated a third time to its melting temperature and then pressed into the final shape. Thermosets are cured at much lower temperatures (120-180°C) and are much easier to manually form into the desired component. Ease of manufacture of thermosets compared to thermoplastics makes them a better choice for low quantity parts.

Due to the unique nature of each space vehicle and the tape springs used in its structure, the assumption is made that a thermoset will be used as the matrix [3]. Themosetting polymers can be broken down into several classes commonly used in structural materials including, "polyesters, vinyl esters, epoxies, bismaleimides, cyanate esters, polyimides and phenolics" [3]. Epoxies are the most common matrix material used and since their strength, toughness, and working temperatures are acceptable for use in a tape spring they make the obvious choice. If lower properties were acceptable, polyester resin could present a suitable alternative due to its lower cost. If higher strength, toughness, or temperature capabilities are required, bismaleimides and then polymides would be considered. Epoxies are used for working temperatures below 135°C, bismaleimides below 177°C, and polymides up to 315°C [3]. Epoxies are commonly composed of various chemical compounds. These differing chemical structures allow for the improvement of material properties above a single compound epoxy. Epoxies also contain curing agents that enable or accelerate the curing of the epoxy. Some of the properties that are commonly enhanced include high temperature behavior, cure temperature and time, uncured viscosity, and moisture absorption [3].

Toughness is a issue with thermoset polymers since they are commonly very brittle. Several methods are possible to improve the toughness of a thermoset. Campbell names four different methods capable of toughening a thermoset matrix composite [3]. The first is network alteration, which is either reducing or extending molecular crosslinks to approach thermoplastic behavior which has no crosslinking. The second is rubber elastomer second-phase toughening, which involves adding rubber particles into the matrix that are of sufficient size and elasticity to halt crack growth parallel to the fibers. The third is thermoplastic elastomeric toughening, which is the inclusion of thermoplastic material into the thermoset. The final method is interlayering, which

involves the insertion of tough layers of material, such as fiber less matrix, in between the matrix layers.

The final property of concern resulting from the matrix material is T_g. T_g represents the point at which the polymer matrix transitions from the glassy regime to an amorphous regime. This transition is represented by a significant reduction in the stiffness, or modulus of the material. T_g is typically below the melting temperature, but exceptions exist. The stiffness reduction is directly tied to the mobility of the polymer chains increasing as the temperature is elevated. This same increase in mobility affects an increase in viscoelasticity of the material.

Tooling.

Tooling is the device(s) that the composite is laid up on and cured to form the desired part shape. It is logical then that the better the tool is, the better the final part. A better tool involves consideration of thermal expansion, composite tension, heat transfer, minimization of fabrication steps, and finally cost of the tool. Thermal expansion considerations include issues arising from the fact that the tool and composite part are typically composed of different materials. It must be ensured that the exact part size is achieved despite the changes in size of the tool. The composite can be over strained in internal tension if the tool expands too much. As the tool contracts on cooling, the composite can also become over strained in compression. The tool can cause significant damage to the composite part if the strain in either direction is too large. Composite tension is a separate consideration ensuring the tool provides sufficient tension to the part so that the directionality of the fibers is maintained.

Heat transfer is the process by which the tool distributes heat to the part within the autoclave. If the tool is of large mass, it can be a significant heat sink to the side

of the composite that is in contact with the tool. This heat sink provides a gradient of temperature over the composite and a resulting gradient in cure. A poorly designed tool can also create non-uniform cool spots over the part causing areas of poor cure or areas of over cure.

Minimization of fabrication steps is a goal for both the tool and the composite. For the tool, minimization of fabrication steps is ideal due to the difficulty of achieving exact dimensions if the tool requires several molding steps. For the composite part, minimizing fabrication involves reducing the number of parts and the amount of assembly required to create the final product. The cost of the tool is a function of the material used, steps to fabricate, precision required, and complexity of the design [3].

For a tape spring, the part is going to be specialized in form for the space vehicle need. This means few tape springs will be created on a single tool, and a less durable tool material can be used. Uniformity of the part in dimension and cure are of highest importance to ensure consistent and reliable deployment and shape. Since a tape spring is a very simple shape, the tool does not need to be complex. It may be simplest and cheapest to use a high precision steel pipe as a tool. For large tape springs, a thin steel arch can also provide an inexpensive and yet dimensionally precise tool that is thin enough to provide uniform cure. Ideally the steel arch would be designed without internal supports that could act as localized heat sinks. A preferred design is to have the steel tool arch supported at the ends of the arch only, and at a sufficient distance from the tape spring part to prevent any thermal affects. Part of designing the tool also includes consideration of the method of combining the fiber and matrix into the thickness and direction desired. This combination is known as lay-up.

Lay-up.

Campbell notes that the cost to lay-up a part can account for 40-60% of the total part cost [3]. Chawla and Campbell discuss several methods of laying up a composite part [3, 4]. These methods include hand lay-up, filament winding, pultrusion, molding, and automated tape and fiber placement. Hand lay-up is the most labor intensive but can create unique and dimensionally complex parts. Hand lay-up is the method by which prepreg tape or fibers are laid down and then the matrix is then 'painted' on. Filament winding is a method by which impregnated fiber or tape is wrapped onto a mandrel. Filament winding is ideal for smooth, round shapes. Automated tape and fiber placement is a method by which a machine is used to perform actions similar to hand lay-up using impregnated tape or fibers. Pultrusion is similar to traditional line manufacturing techniques where the composite fibers are pulled through a guide, impregnated with matrix and cured in one continuous line. Pultrusion creates one long, dimensionally consistent part. Molding is similar to plastic mold manufacturing where a fiber form is placed in a mold and injected with the matrix material. Molding can create complex shapes in a highly automated fabrication methodology. Both pultrusion and molding cure the part as it is created where the remaining methods typically use an autoclave to achieve the conditions necessary to cure the part [4].

The methods that can produce a tape spring shape include hand or automated lay-up, filament winding, and pultrusion. To program an automated machine or create a pultrusion line is prohibitively expensive for the low runs expected for space based tape springs; however, these methods could create tape springs with greater uniformity. Uniformity of the tape spring is critical for a consistent deployment and final shape of the space structure. Hand lay-up using a prepreg tape stands out as the inexpensive choice for the unique low number production of tape springs and should provide sufficient uniformity for the application. Uniformity of the composite is also

impacted by the cure.

Cure.

For a hand lay-up using prepreg tape, curing is traditionally performed in an autoclave. The autoclave subjects the composite to elevated pressure and temperature to achieve a successful cure. During lay-up, a process called debulking is performed during which the fibers are vacuumed together at intervals of typically 5 or more layers of tape. Each tape is exposed to the environment where it can collect particles on its surface, those particles along with air pockets (voids) between the layers of tape make for poor contact between the tape. Debulking is performed to better compress the plies together which reduces voids and contaminants found on and in between plies. Debulking can also be performed at elevated temperatures to aid in the removal of the contaminants and voids.

An issue of major concern during curing is determining the amount of pressure applied to the matrix material. If the matrix material is sufficiently sparse, it is possible for the fibers in the composite to carry all of the pressure. If the matrix experiences zero or negative pressure during cure, voids and precipitates are prone to form. These defects greatly reduce the engineering properties of the material. Structural composites are typically made to maximize the percentage of fiber contained. The goal of high fiber fraction and uniformity of the matrix are in conflict and must be optimized. Older composite curing cycles contained an initial ramp to an intermediate temperature that allowed excess resin to bleed out prior to the main cure. More modern techniques use only the desired final amount of resin, called net resin, in the composite and do not require bleeding of excess [3].

The curing cycle for a thermoset prepreg is typically specified by the prepreg manufacturer. For instance the pre-preg manufacturer, Patz provides for its F7 resin

the recommended cure cycle shown in Figure 3 [20]. Patz recommends the prepreg be cured at the autoclave max pressure, which Campbell states is commonly around 100 psig.

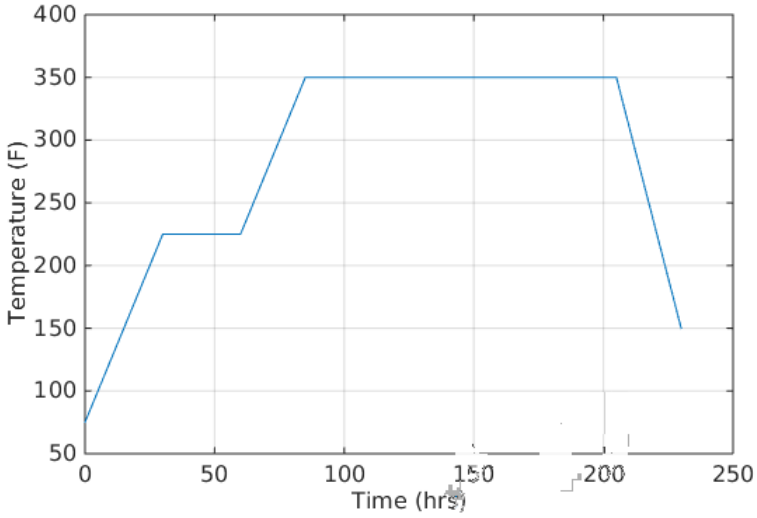

Figure 3. Cure Cycle Recommended for Patz F7 Prepreg

Commercialization and Assembly.

Commercialization is defined here to pertain to mass manufacture, where increased quality and decreased cost are primary concerns. For the tape spring materials chosen, this primarily changes only the method of lay-up and cure. As expressed earlier the major driver for hand lay-up was the uniqueness of the tape spring and the low production numbers. For larger production numbers, the ideal method of production involves a combination of pultrusion and filiment winding. In this production method, the fibers are impregnated and wound around a tool as it is being pulled trough a forming and curing die. The tape spring is made as a cylinder that is then cut at the end of the production line into two separate tape springs. The more complex production method would require significant investment to develop and would only be reasonable for large production lots.

Assembly of the tape spring to the space vehicle can have significant impact on its reliability. Mechanical means of assembly including fasteners or straps are not recommended for composite tape springs as they create highly localized stress points that can lead to failure. A preferred method is to bond the tape spring into a shaped fixture utilizing adhesive. If stresses in the tape spring at the tip of the fixture are too severe, reinforcement thickeners can be added to this root section of the tape spring. These thickeners will add to the deployment force and this resultant force must be taken into effect [3].

Composites Summary.

In review, one proposed design for a spacecraft tape spring utilizes a quartz fiber and epoxy matrix. The tape spring should be layed up by hand using prepreg tape on a simple steel tool. Curing should be performed to the prepreg manufacture's recommended cure cycle in an autoclave.

Due to the use of a polymer matrix, the tape spring properties are more dependent on time than traditional structural materials. Time dependent material properties include: the age of the prepreg before cure, the lay-up method, the cure uniformity and time, and the environmental conditions throughout the parts fabrication and transport. The storage of the tape spring throughout its life cycle is critical to this time dependent history. The careful consideration of the effects of these steps is paramount to achieve a desired design outcome. Having thoroughly reviewed the materials and manufacturing methods both in use and of potential to produce tape springs it is important now to discuss how this material will behave over time.

2.3 Time Dependent Effects

There are many time dependent properties for every material. The focus of this thesis is on those properties which can effect deployment of a tape spring after storage. The tape spring is expected to be stored primarily in the rolled configuration. Gates provides a helpful division of the major types of aging as chemical, physical, and mechanical [6]. White also adds the consideration of weathering effects, which are simply a specific form of chemical aging [28]. Considering environmental effects on the tape spring once deployed is beyond the scope of this study.

Measuring the aging of the tape springs used in this thesis is out of scope; however, it is important to understand these behaviors since they are linked to the creep and stress relaxation behaviors. For the purposes of this thesis the aging of most concern is physical aging (or the progression towards equilibrium experienced by all glassy polymers) [25]. Corrosion (chemical) and fatigue (mechanical) will not be considered in detail as the fabrication and storage environments are assumed to be benign in these areas.

Creep is the decrease in strain in a material under a constant stress. A similar behavior to creep, called stress relaxation, is the decrease in stress of a material subjected to a constant strain. Creep and stress relaxation are physical aging responses to a load history. Viscoelasticity is the material property of the matrix that allows creep or stress relaxation to occur which is characteristic of polymers. The time dependent effects on the fiber are expected to be orders of magnitude less than the matrix material due to both the material properties and the protection afforded the fibers by the matrix [27].

Physical Aging.

Physical aging includes those effects that depend on the environmental interactions with the material, instead of the physical configuration and loading. For the composite, this includes the evolution of the matrix "characterized by changes in the free volume, enthalpy, and entropy of the polymer" [6]. Often this includes events such as post-cure and oxidation. This aging is important as Sullivan puts it "without physical aging many glassy polymers could not be used to make load bearing structures" [27]. His reasoning is that physical aging increases the stiffness of the polymer preventing loaded polymers from deforming to failure. Understanding of the physical aging properties requires temperature tests and utilizes the time-temperature superposition principle [6, 8, 12, 13, 25, 26, 27, 28]. Temperature tests necessary to use the time-temperature superposition principle are not performed in this thesis; however, the tests performed in this thesis are identical to those performed to use the superposition principle if the tests are performed at various temperatures.

Creep and Stress Relaxation.

As an amorphous material, polymers in their relaxed state represent and overall random ordering of polymer chains. Creep or stress relaxation induces a straightening or crystallization of the polymer chains at the microscopic scale. Creep and stress relaxation tests have shown that common material behavior fits into three regions: primary, secondary, and tertiary shown for stress relaxation in Figure 4. This thesis will assume no tests reach the tertiary region, where failure of the material occurs.

Creep and stress relaxation are commonly represented using rheological models. For stress relaxation, the simplest model with good results is the Maxwell model. The Maxwell model is represented by a spring and damper shown in Figure 5. The spring constant is labeled E, and the damper value is labeled η. Using the following

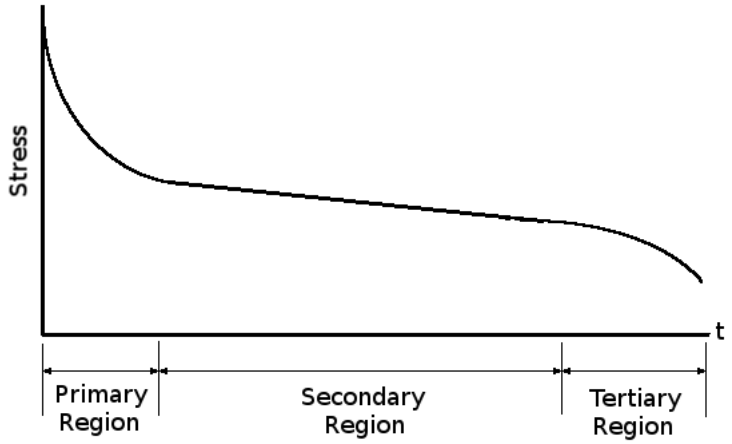

Figure 4. Typical Stress Relaxation Curve

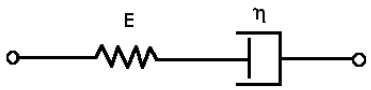

Figure 5. Linear Maxwell Rheological Model

derivation, a simple equation is obtained to use in fitting stress relaxation data. Equation 1 is taken from Shames equation 6.20 showing a Maxwell representation for a relaxation test. ε_0 is the initial induced strain, E is the modulus of elasticity, the ratio (η/E) is the relaxation time, and $[u(t)]$ is the strain loading function.

$$\tau(t) = \varepsilon_0 E e^{(-E/\eta)t}[u(t)] \tag{1}$$

Equation 2 is taken from Shames equation 7.1 showing the modification required when considering the nonlinear behavior of creep. In Equation 2 the strain at any time $\varepsilon(t)$ is the sum of the elastic strain component ε_e, the steady creep strain component $\varepsilon_s(t)$, and the transient creep strain component $\varepsilon_t(t)$ Equation 2 holds true the same with stress replacing strain. For detailed derivation of the Equations 1 and 2 please reference Shames and Cozarelli [24].

$$\varepsilon(t) = \varepsilon_e + \varepsilon_s(t) + \varepsilon_t(t) \tag{2}$$

Combining Equations 1 and 2 results in Equation 3. Since u(t) shown in Equation 1 is constant for $t > 0$, it is dropped from Equation 3. Here β represents the elastic stress response, and ε_1 and ε_2 represent the strain induced on the specific term or path as shown in Figure 6.

$$\tau(t) = \beta + \varepsilon_1 E e^{(-E/\eta)t} + \varepsilon_2 E1 e^{(-E1/\eta)t} \tag{3}$$

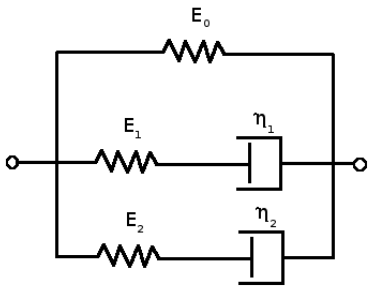

Figure 6. Non-Linear Maxwell Rheological Model

2.4 Standards of Note

The Department of Defense has created a handbook series that deals with standardizing composite tests and methods, MIL-HDBK-17. These test methods are useful for determining the basic material properties; however, they are not applicable to the unique properties that provide deployment force in tape springs. Specifically, tests concerning creep and stress relaxation are given heuristic advice but few specifics. The heuristics given in MIL-HDBK-17-1F *6.11 Viscoelastic Properties Tests* will be considered when designing the test methodology [16].

2.5 Similar Studies

Studies that have been performed detailing both the deployment of tape springs, and the aging of composites will be discussed. A review of these studies will provide the background needed to understand what type of tests are necessary for understanding the internal behaviors of the tape spring. The definitive text on composite physical aging was written by Struik [25]. Struik's book entitled "Physical Aging in Amorphous Polymers and other Materials" was published in 1977. In his book, Struik adapts the basic theories of aging and creep behavior to provide a methodology for determining aging effects of polymer matrix composites using experimental data. He also provides experiments to be performed to discover the specific aging properties of any composite material of interest. Struik's work demonstrates an increasing stiffness and corresponding decrease in creep and stress relaxation rates as a polymer ages. Several authors have since expanded upon Struik's work [8, 26, 27, 28]. These authors validate Struik's work and expand the known limitations to the model. The work by Sullivan proving the applicability of these theories on resin matrix, glass fiber composites is particularly applicable [26, 27].

Kwok and Pellegrino in "Viscoelastic Effects in Tape-Springs" and their follow-on work, "Folding, Stowage, and Deployment of Viscoelastic Tape Springs" investigate the effect of folding and stowage on the deployment of tape springs, similar in principle and purpose to this thesis [12, 13]. Tape springs were created by re-forming a thermoplastic material into a tape spring shape. The tape springs were compressed as shown in Figure 7 by a Instron testing machine. The Instron test machine is used to create a strain profile during which the resulting stress is measured. Stress during the entire strain cycle is measured from un-deformed through a final fixed strain condition during which relaxation occurs. The fixed strain condition was induced for a little under an hour and a half. The results showed a 50% decrease in resistive force during

the stress relaxation. The paper also shows the successful correlation of a model with the experimental behavior using viscoelastic theory implemented in Abaqus software. The authors discuss the difficulty in predicting the experimental results with models. A discovered solution is the incorporation of manufacturing defects into the model. The importance of considering manufacturing defects on tape spring stress relaxation results is made clear by Reynolds [21]. This thesis focuses on a production representative tape spring design utilizing a thermoset resin matrix, where Kwok and Pellegrino use a tape spring specifically made to exemplify the behavior of interest.

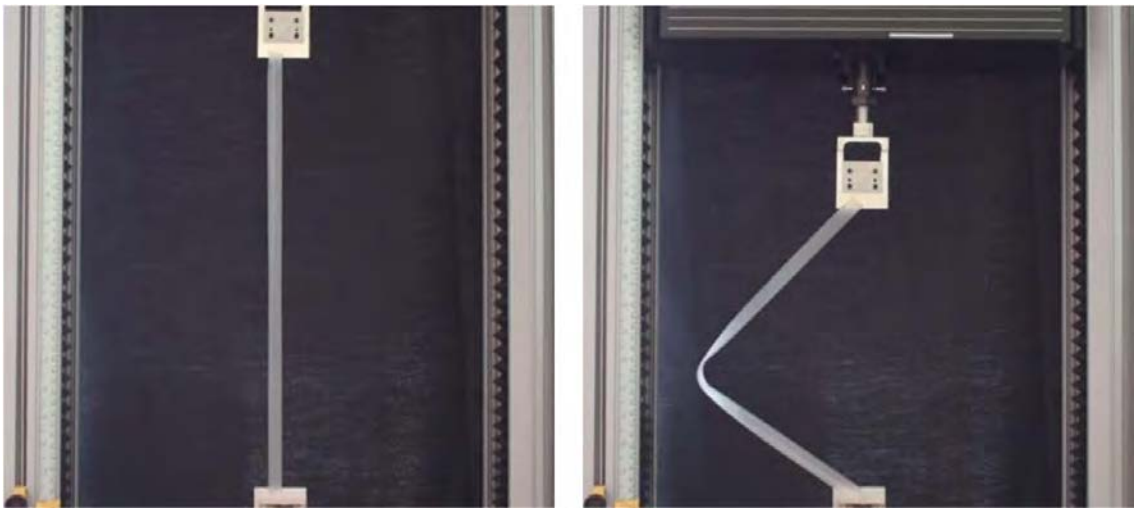

Figure 7. Bend, Fold and Hold Test Setup [12]

Jennings, Black, and Gutierrez have provided a modern theory on tape springs in "Geometry and Moments of Bent Tape Springs" [10]. This theory is critical to understanding and modeling the behavior of tape springs based on the shape. Combining the static and dynamic values obtained with time variance of shape can add a prediction method of the effects of tape spring aging using finite element modeling (FEM). Several tests have been performed on the tape springs of interest prior to AFIT involvement. AFRL/RVSV performed two experiments with tape springs [21, 22]. The first examined the dependence of the temperature of the tape spring on the deployment speed. The second measured the creep of a stowed tape spring.

AFRL/RVSV also provided the glass transition temperature (T_g) test results from the manufacturer.

The deployment speed dependence on temperature showed drastic differences. At high temperatures of approximately 50°C, deployment occurred in under a second. At room temperature, deployment is on the order of 5 minutes. While at low temperatures of -18°C, deployment took approximately 3.5 days [22]. This drastic difference shows the potential for unpredictability in deployment speed and ability. Figure 8 shows these test results.

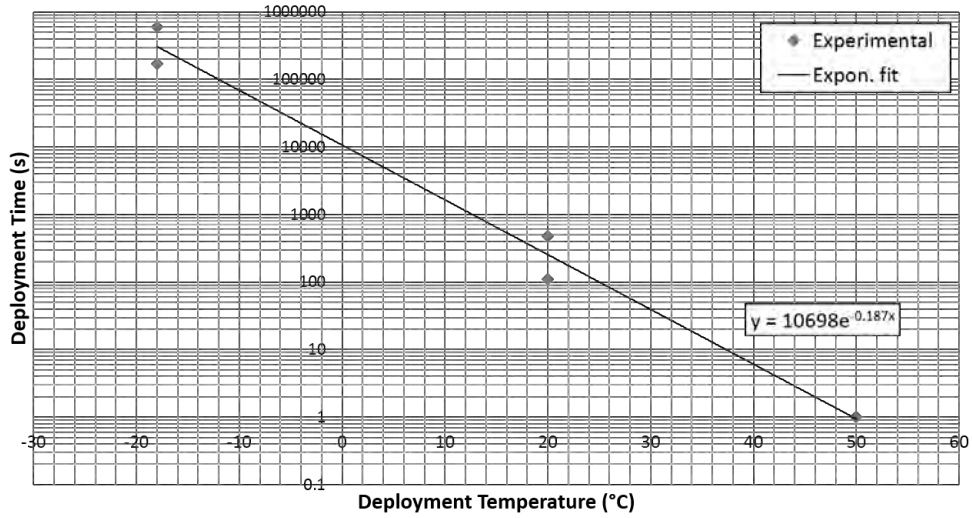

Figure 8. Deployment Speed for Various Temperatures [21]

The creep test performed by AFRL/RVSV was conducted by rolling six tape springs and then storing them in a controlled environment at 29.5°C. At monthly intervals one tape spring was removed and deployed. A measurement of the radius of curvature of the cross section was made before storage and after deployment. These radii of curvature were compared and taken as a representation of creep behavior. Recovery of two months was also performed on each tape spring sample. This test shows that storage time has no effect on creep and that radius of curvature progresses toward a return to the original shape over time once deployed. Reynolds concluded

from these results that manufacturing variability has a greater effect on deployment than aging [22]. Manufacturing variability could affect the shape, internal stresses, and defect concentration. While this variability may have a large effect, it is still critically important to discover what the aging outcomes are and consequently how they affect the deployment of the tape springs.

The manufacturer provided T_g test results are shown in Figure 9. The figure shows Patz F7 has a T_g of 200°C [19]. T_g is predominantly a property of the matrix component of the composite and a byproduct of the matrix being a plastic material. All plastics have a glass transition temperature. For temperatures above T_g the plastic loses a significant portion of its stiffness and becomes more viscous.

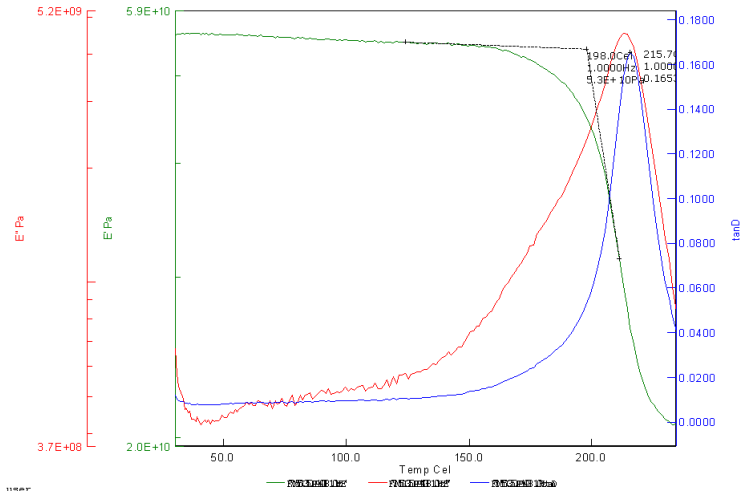

Figure 9. Patz T_g Test [19]

2.6 Summary

Manufacturing variances are expected to be of great significance [12, 21]. It is critical to maintain a record of the time history of each tape spring sample from fabrication through final test in order to account for physical aging effects. The specific design of the tape spring tested in the current work is created to have the deployment force provided by the fibers should the matrix lose the strain energy

required for deployment. This design is expected to result in a folded force that will not approach zero but approach an asymptote that is equal to the force supplied by the fibers.

Many studies have been performed on the aging of composites and on the behavior of tape springs. The merging of these two studies must be completed to understand how the physical aging of the tape spring will affect its behavior. Typical structural materials have simple loads applied to them. The tape spring is unique from typical structural materials as it uses stored internal energy which is released to perform a function of the space vehicle. The papers by Kwok and Pellegrino, summarized in Section 2.5, begin to address the modeling and experiments necessary to address this problem [12, 13]. This thesis will attempt to explore the reproducibility of their results as well as extend the tests to more complex and production representative tape springs. This thesis will not look at the entire cycle, particularly folding and deployment will be outside the scope, the focus is on stowage. Using the theory and previous experiments outlined above a method to test the stress relaxation and physical aging effects during storage of tape springs will be developed.

III. A Method for Determining Stress Relaxation in Rolled Tape Springs

After careful review of the current body of knowledge, a testing schema was developed to acquire the data necessary to sufficiently answer the questions posed in Chapter I. This chapter discusses the data needed as well as the method for collection and analysis of these data. A discussion of what data are needed begins the chapter in Section 3.1. Following are several sections discussing the setup used to acquire these data beginning with Section 3.3. Methods are then discussed beginning in Section 3.5 including process, and procedures. A discussion of the equipment setup and calibration will follow beginning in Section 3.2. Alternatives are reviewed in Section 3.8. Finally, the methods used to analyze these data will be discussed in Section 3.9.

3.1 Data Necessary

An investigative path must be laid out to sufficiently measure and understand how stowage of tape springs effects deployment. As mentioned in the assumptions in Chapter II, the scope of this thesis will not include actual deployment tests. It is necessary to gain a more fundamental understanding of the problem before deployment correlation can be made to tape spring aging in the stored configuration. Several changes can be expected to produce measurable results as a tape spring ages. Chemical changes can be determined via spectroscopy as well as change in mass. Mechanical changes can be measured by the many different non-destructive testing methods used in the field of fracture mechanics. Physical aging is best determined by creep or stress relaxation tests [6]. The simplest method to determine the aging behavior of a stowed tape spring is to measure the stress relaxation via a measurement of the change in force over time of a strained tape spring.

The tape spring provided by AFRL is quasi bi-stable, meaning it is not bi-stable

immediately after production but becomes bi-stable after being rolled for a period of time. Bi-stability is a concern because it calls to question whether the rolled condition can be sufficiently represented by a folded tape spring. Bi-stability is caused by a balance of forces between the fibers and the matrix that creates a low energy point when completely rolled [9]. The quasi bi-stability of the tape springs provided by AFRL is due to the ± 45 layers. This layup means that forces applied across the tape spring create a shear force completely concentrated in the matrix. Peterson goes into detail as to the effects of the particular layup, how the the shear force is caused, and test setups to characterize this behavior [20]. The result of bi-stability is when you roll the tape spring completely, it stays rolled. It is assumed that the matrix will suffer stress relaxation of the same order when folded over in the test configuration as it would when rolled; however, the test load is not expected to reach zero like a bi-stable case. Later work will be required if the bi-stability is to be properly addressed; however, it is logical to say that in any situation the bi-stability should present nearly the same or slower stress relaxation response because the bi-stability does reach zero and thus no further relaxation is occurring. The higher the level of stress relaxation the greater concern to space vehicle designers. Any test between the bi-stable stress free zones (fully open and rolled) should represent a worst case storage condition. Since the rolled tape spring does not present any measurable force in the rolled configuration due to its quasi bi-stability, unique test procedures must be devised to replicate the loading of the rolled tape spring.

Along with the stress relaxation results, data on the change in physical shape will be obtained. Understanding any changes in shape will allow a better understanding of the lasting effects of stowage on tape spring. These data are necessary for better correlation of a FEM model with the experimental results. An added benefit of shape testing is that it is a non-intrusive method of measurement.

3.2 Equipment

AFRL/RV provided the necessary tape spring samples to be used in testing. Consideration will be given to production, storage time, and storage conditions experienced by each sample. The tape springs are made of a quartz fiber/epoxy resin matrix composite with a $\pm 45/0/\pm 45$ layup. The ± 45 layers are made of Astroquartz 525 fiber with a PMT F7 resin matrix and the 0 layer is made from S2 glass fiber and the PMT F7 resin matrix. Six samples, each five feet in length, were provided at the beginning of testing. After manufacturing, samples remained in the extended shape and were not folded or pressed until the test began unless otherwise noted.

One ATI NANO 43 load cell, Two Cooper LGP 312 pancake load cells, and a Modern Machine and Tool six component wind tunnel balance (WTB) are used as force measuring devices. There are two test setups. In the first test setup the NANO 43 and LGP 312 cells are attached to a National Instruments NI USB-6259 data acquisition system which connects to a desktop computer running LabView 2013 32-bit via USB. The NANO 43 is powered by its own supply, provided by ATI. The LGP 312 cells are powered by an HP 6236B triple output power supply set to 10V and providing 0.05 amperes. In the second test setup, the wind tunnel balance is connected to a National Instruments NI PXI-1050 chassis via a NI SCXI-1314 terminal block. The chassis runs Windows XP and LabView 2010.

Three pin temperature sensors are used at each test setup and are hooked into the NI USB-6259 and NI SCXI-1314, respectively. The temperature sensors output in voltage, and since the only concern is changes in temperature, no attempt is made to determine the temperature correlation to the voltage.

The ATI NANO 43 and wind tunnel balance measure load forces in six dimensions. The tests have been set up one dimensionally, meaning of the six dimensions available only direct compression is of concern. The LGP 312 has an single output voltage that

Sensor	Accuracy	Range
ATI NANO 43	0.0078 N	0-36 N
Cooper LGP 312	0.089 N	4.5-44.5 N
MMT Balance	0.001 N	0-17.8 N
FARO Arm	0.06 mm	N/A

Table 1. Sensitivity of Measurement Devices

varies based on the input voltage and force applied. The maximum voltage allowed, 10V, is used to ensure maximum change in output voltage for change in force applied. The shape test is performed utilizing a FARO arm connected to a laptop running Innovmetric PolyWorks v11. Table 1 presents the published accuracies of the sensors used.

3.3 Setup to Measure Stress Relaxation

Measuring stress relaxation in a rolled tape spring presents an interesting challenge, especially for one that presents bi-stability. An attempt must be made to locally replicate the shape of the rolled configuration without inducing uncharacteristic forces or strains. Equally as important is the ability to measure the force. The tape spring deployment force is low, between 0.3 and 0.4 Newtons, and these small forces require highly sensitive measurement. Two methods of test are explored in this thesis.

The first method is compressing a small portion of tape spring to nearly flat and measure the reduction in the flattening force required over time. This test is chosen as it takes around 20 N to compress a one inch portion of tape spring. This allows the use of less sensitive load cells as a larger force makes greater changes over time for the same percentage of stiffness change.

The second method is folding the tape spring to achieve a locally flat portion in the bend and measuring the reduction in force required to hold this fold. The folded

test is most similar to the test performed by Kwok and Pellegrino [12, 13]. The folded test advantage is that it closely replicates the rolled shape of a tape spring locally. The primary disadvantage is that the force to hold the fold is very small, around 0.3 N. This small force requires a highly sensitive load cell.

Temperature probes are used to measure the ambient temperature during each test. These data allow the correlation of the temperature with the changes in sensor output. Temperature and load data are output at equal intervals.

Flat Test.

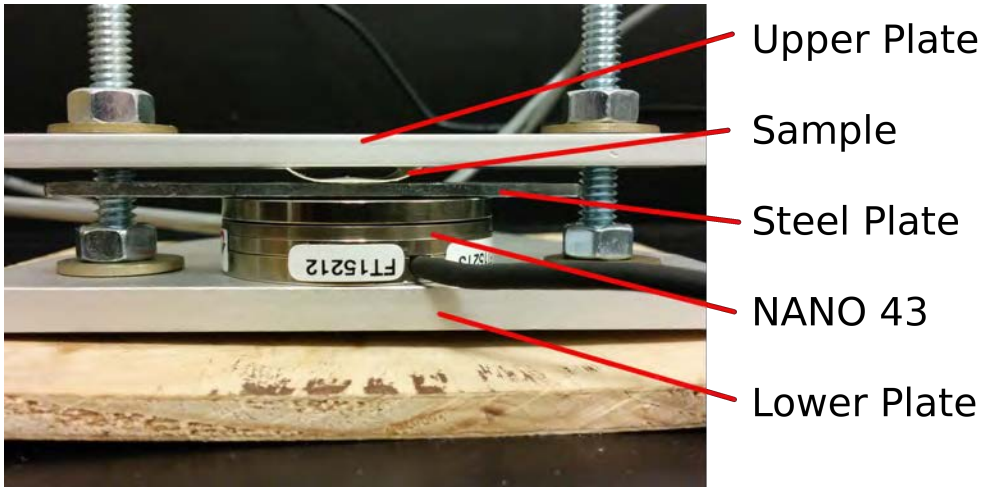

Figure 10. NANO 43 Flat Stress Relaxation Test Setup

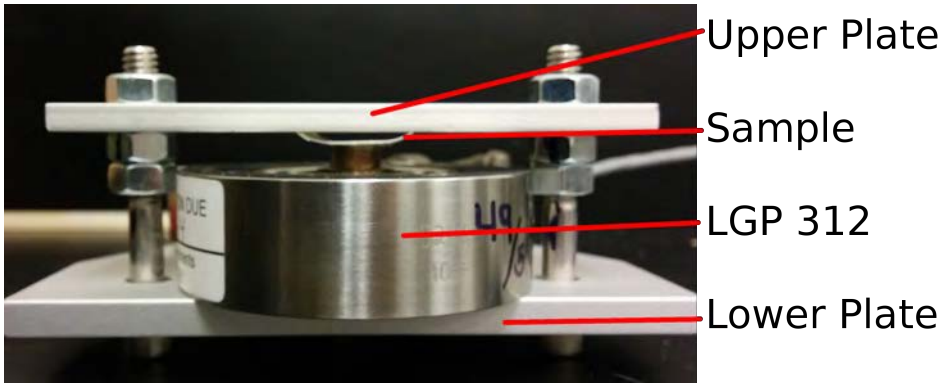

Figure 11. LGP 312 Flat Stress Relaxation Test Setup

In order to capture flat stress relaxation, an apparatus is required that pinches the tape spring flat against a load cell. Two bolts are used to pinch the tape spring and the load cell between two aluminum plates. The setup pinches the entire tape spring sample. The NANO 43 is circular in shape with a whole in the middle requiring an additional steel plate be used between the tape spring and the upper aluminum plate in order to spread the load evenly and prevent excess torque. The plate also allows for force on the tape spring to be applied to the entire sample. The flat test with the NANO 43 is shown in Figure 10. For tests utilizing the LGP 312, the sample is placed with the rounded face toward the button of the sensor. The button directly contacts the tape spring and provides a smaller round force profile. The flat test with the LGP 312 is shown in Figure 11. The flat stress relaxation test will be performed at a nearly fully flattened state as shown in the test figures.

Folded Test.

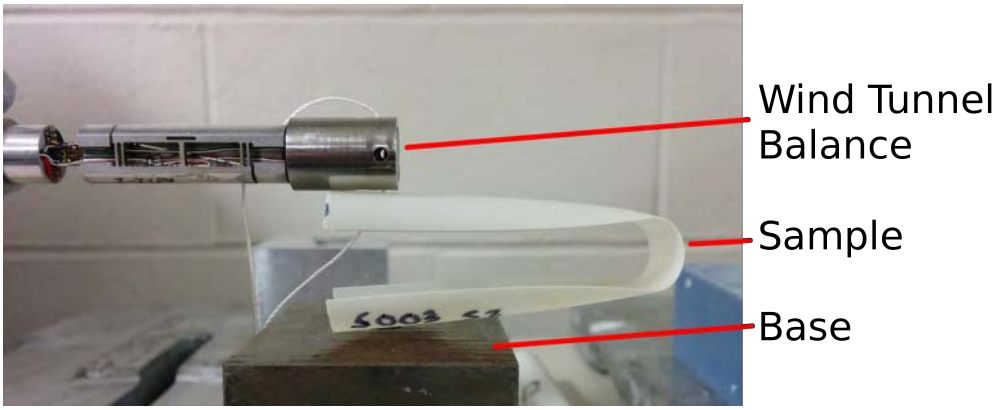

Figure 12. Folded Stress Relaxation Test Setup

In order to capture folded stress relaxation, an apparatus is necessary that holds the tape spring folded at a constant strain. Ideally, the same setup would be used as the flat test but pancake sensors available did not have a sufficiently high resolution to capture the low forces exhibited in a folded test. A Modern Machine and Tool

wind tunnel balance is used to achieve the sensitivity necessary. The wind tunnel balance is mounted to a fixture and steel blocks provide a base creating a gap of fixed size. Friction is used to hold the tape spring in place. The fold will allow the ends of the sample to be in their relaxed state. This setup is shown in Figure 12.

3.4 Shape Test

Figure 13. Shape Test Setup

The final test setup is the shape test. The primary energy in tape springs comes from the distortion of the shape. In order to gain understanding about how the changes in internal stress effect the shape, a measurement is made of the change in shape over time. The measurement arm is mounted to a marble top on which the test is performed. The sample apparatus base is an extruded piece of aluminum with squared ends. To this base is bolted on aluminum squares that can be tightened to the base. The test fixture is secured to the marble base. The tape springs are folded in three locations with the open ends compressed in between the base and the squares of the fixture. The test fixture with mounted tape springs is shown in Figure 13.

3.5 Methodology of Test Performance

The flat tests will be run utilizing the following procedures. A one inch sample is labeled and cut from a tape spring. Data collection is initiated in LabVIEW with the load cell unloaded. The NANO 43 is biased to zero. The sample is loaded onto the sensor and then the top plate is pressed down by tightening the bolt on each nut. The tightening is complete when the tape spring just begins to create an M shape and bend in the middle. This bend occurs when the height is just under 2 mm. The flat stress relaxation test is then run for two days. After the test is complete, the sample is unloaded and then the data collection is stopped.

The folded stress relaxation test will be performed similar to the flat stress relaxation test. Tape spring samples will be labeled and cut to five inches in length. The wind tunnel balance will begin unloaded. Data collection is initiated in LabVIEW and then the sample is folded by hand and placed in the gap between the sensor and the base. The folded stress relaxation test will be performed for three days. After the allotted time the sample is removed from the test and allowed to unfold and recover for 60 seconds. The sample is then folded and is returned to the gap between the sensor and the base for retest. It is expected that unfolding may rejuvenate the samples. The samples for each test will be taken from various lots of the tape spring supplied by AFRL.

The shape test will be performed utilizing the following procedures. A six inch sample is labeled and cut from the tape spring. The tape spring is folded and placed in the test fixture. Each test sample is loaded and then scanned immediately. After the first sample is loaded and scanned the clock starts and additional scans are taken at minutes 10, 20, 30, 45, 60, 90, 120, 200, 320, 530, 1390, 2830, and 7150. The next sample is loaded immediately after the previous sample is initially scanned. Each sample is scanned at the same intervals as the first sample.

3.6 LabVIEW Program

For the wind tunnel balance a previously existing LabVIEW program was modified to output the desired results. This program outputs a mean value of measured samples and records at 0.2 Hz.

For the NANO 43 and LGP 312 cells a LabVIEW program was adapted from an ATI provided code. The NANO 43 has a set of six output voltages that are not independently related to any specific axis. The ATI portion uses a calibration file to correctly read these voltages and output the measured values. The setup in LabVIEW also allows biasing of the data. Along with the NANO 43 data the LGP 312 output voltages, HP 6236B power supply voltage, and temperature sensor voltages are also read into LabVIEW. Measurements are taken at 10000 Hz then averaged every second to output at 1 Hz. A time value is stamped on each output line and all the data is written to a text file. Simultaneous collection is performed to minimize the data collection equipment necessary and maximize the simultaneous tests performed.

3.7 Sensor Calibration

Several sets of tests were required to determine the sensor behavior over time and during changes in temperature in order to remove the sensor behavior from the stress relaxation measured. To test for sensor creep, a mass is placed on the sensor, ideally the mass is close to the force to be measured. The mass is left on the sensor for a period of time similar to the length of test. Figure 14 shows the NANO 43 and wind tunnel balance loaded with a 20g mass For the NANO 43, this mass is placed directly on the sensor, for the wind tunnel balance the mass is strung from a fixture hold at the end of the balance. Figure 14 also shows the NANO 43 and LGP 312 cells with a 100g mass applied. Like the NANO 43, the mass is placed directly on the LGP 312. A final test is done to understand the sensitivity of the LGP 312 compared to the

NANO 43 where masses of 20g, 50g, 100g, and 500g are placed on the sensors. The resulting force reading from each sensor is shown in a subplot at each mass in Figure 15.

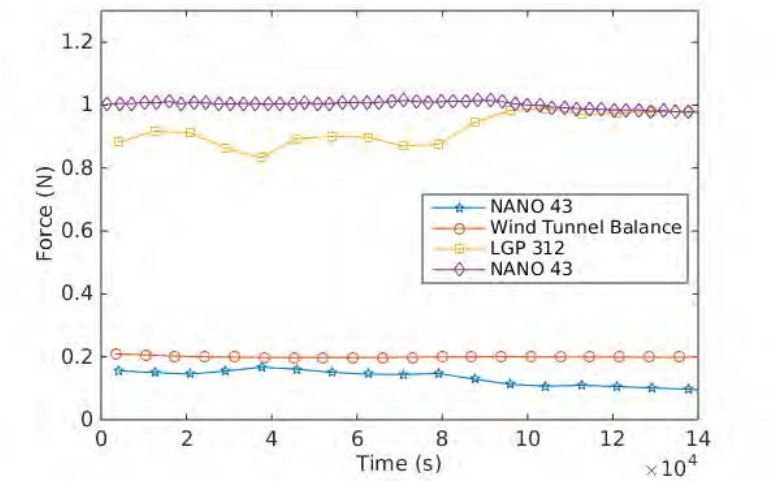

Figure 14. Constant Load Tests at 20g and 100g

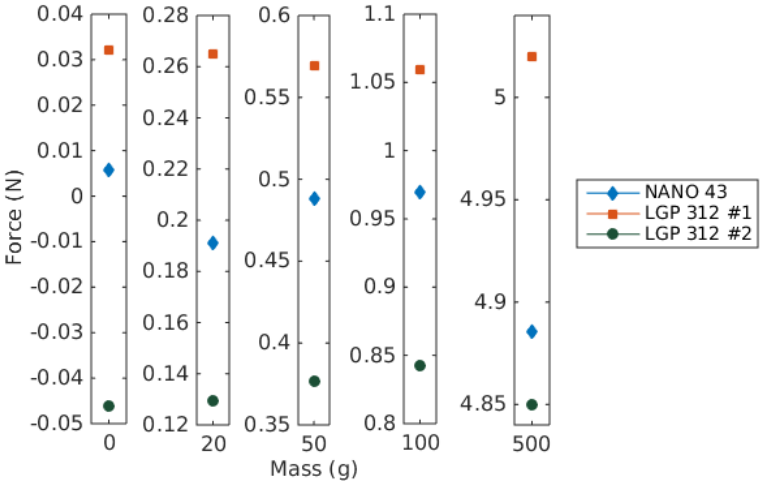

Figure 15. NANO 43 and LGP 312 Variable Load Test

Along with the sensor creep tests, tests were conducted to create minor variances in temperature so temperature sensitivity of the sensors could be determined. These temperature variances were first noticed as an issue during the preliminary sensor creep tests as can be seen in Figure 16. The temperature tests were conducted with

a constant mass applied similar to the sensor creep tests. The temperature variance on the wind tunnel balance is shown in Figure 17. To correct for the temperature a temperature correction factor was created by fitting a line to the temperature to force data obtained from these tests. The correction factor was then applied to rotate this line so that the force measured was constant with changes in temperature.

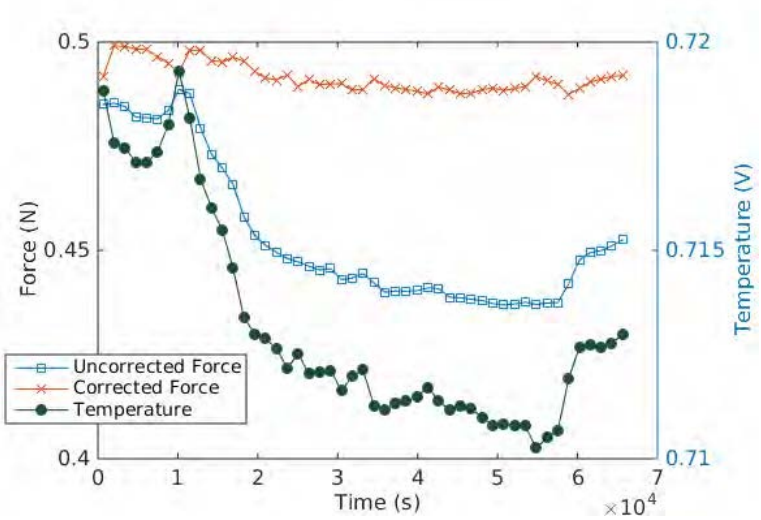

Figure 16. ATI Temperature Variance 50g Constant Load

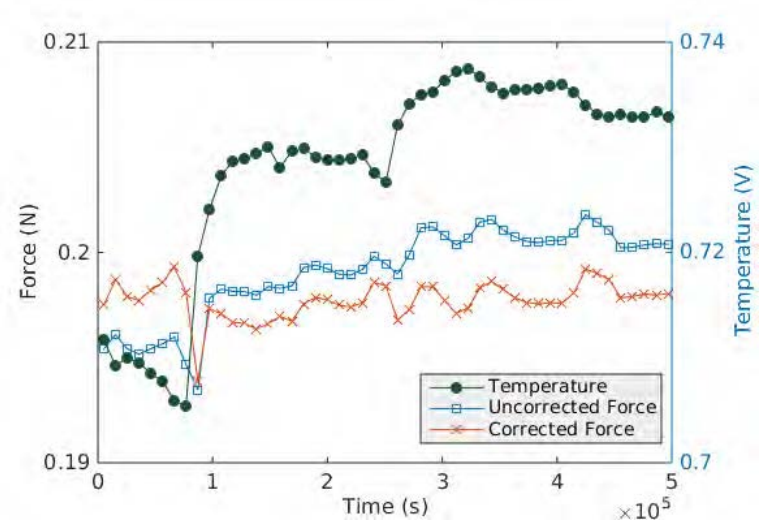

Figure 17. Wind Tunnel Balance Temperature Variance 20g Constant Load

3.8 Other Possible Solutions

Several methods of holding the tape spring are possible. The designs that provided the specific load required for each test but were the simplest to construct were chosen. The tape springs could also have been secured at each end and folded similar to what was done by Kwok and Pellegrino; however, the equipment necessary for this method was not available [12, 13]. To create a similar fixture also raised concerns about friction and other effects that could corrupt the test. The amount of fold to induce is also variable. Because the folded test setup used for this thesis does not clamp on the ends of the tape spring, it proved simplest to fold the tape spring until the ends were parallel. Due to the physical nature of tape springs the bend caused by the fold is assumed to form a radius consistent with the properties of the particular tape spring. The assumption is that this radius does not change despite the amount of fold, but is a property of the material. The work by Jennings lends credibility to this assumption [10]. The region where the tape spring goes from flat to its curved shape is what causes the force to further unroll or unfold the tape spring and is assumed to remain the same no matter the degree of fold chosen. The length of tape spring used in the folded tests is sufficiently long that the ends are distanced from the transition area. The long sample removes any potential edge effects and allows the assumption of a sample of infinite length. Another alternative is to measure the change in radius of the bi-stable tape spring in its rolled configuration. This change in shape would be caused by the relaxation of the matrix which would result in the force of the fibers increasing the bi-stable radius. This change was determined to be too minute to attempt to measure.

3.9 Method of Analysis

The data produced by the load sensors will be analyzed using various mathematical methods in MATLAB. Initially all the data outputted from LabVIEW is taken from the text files and placed in variable cells. Each stress relaxation test as performed will contain the loading and unloading period. Since this data is not desired in the relaxation plots it is removed. Removal is performed by first removing all negative, zero, and very low values (<0.01 N). Then the force and time data is converted to log-log space. A linear fit is made to this data and points greater than 10 percent from the fit are removed, this solely removes the initial strain loading noise. Finally, the peak remaining value is made the starting point of the relaxation data. In order to reduce the number of data points to aid in calculations, a windowing average is performed. The number of data points desired is selected and the corresponding window size is calculated and used. Each window is averaged to a single data point. A sliding window smoother was also attempted that takes several points before and after each point and averages them. The smoother was not used on the data or results shown in this work. In order to create a fit to the stress relaxation data, Equation 3 from Chapter II is modified and used as shown in Equation 4. The equation is input to the MATLAB fit function to solve the five variables a_0, a_1, a_2, b_1 and b_2. The 100000 included in the denominator of the exponential is included to scale the b values. The a_0, a_1, and a_2 values represent the general location of the curve, while b_1 and b_2 values represent scaled inverse of the relaxation time for the primary and secondary stress relaxation regions. See Appendix A for the MATLAB code used for the flat and folded tests.

$$Fz = a_0 - a_1(1 - e^{-b_1 * t/100000}) - a_2(1 - e^{-b_1 * b_2 * t/100000}) \tag{4}$$

Two methods are used in analyzing the shape data. The data are partially reduced in PolyWorks with additional analysis done in SOLIDWORKS. For the first method of analysis, PolyWorks is used to cut out the unnecessary portions of the raw scan data. Then each tape spring is exported as a '.stl' file. This file is imported as a surface into a SOLIDWORKS part file. The SOLIDWORKS parts are combined into an assembly allowing a visual representation of the changes in shape over time. For the second method of analysis, PolyWorks is used to create curve over the length of the sample of interest. The curve is used to create cross sections of the tape spring along the region of interest. These data are output as '.txt' files containing the point clouds of the cross sections. The point clouds are then analyzed using the Taubin method to fit the ellipse cross sections and then comparing the ellipse values to determine changes in shape [10]. See Appendix B for the MATLAB code used for the shape test.

3.10 Summary

The methods of collection and analysis of the data to be used in this thesis has been discussed. Consideration has been made at reducing the impact of the sensor variation on the test results. Data are collected from three test setups: flat, folded, and shape. The data are collected and analyzed using MATLAB, PolyWorks, and SOLIDWORKS. These data provide a greater insight into the stress relaxation of tape springs when deformed representative to rolled configurations. The results of these tests as well as implications will be discussed in the following chapters.

IV. Collected Data

The results of the tests accomplished are detailed in this chapter. As with most tests, difficulties arose in the availability of equipment and space. Forty-one tests were completed over a time period of six months. Table 2 lists out the sample designations along with the length and type of test performed on each of the samples. The serial number (SN) represents which tape spring, of the six provided by AFRL/RV, the sample is taken from. The sample number (#) is the designation given to each sample. Flat test samples are one inch in length and given a letter designation. The folded tests samples are five inches in length and designated by the prefix 'S' then followed by the number of the sample in the order it was taken from the specific SN tape spring. The shape test samples are six inches in length and designated by the prefix 'L' then followed by the number of the sample in the order it was taken from the specific SN tape spring. The sample SN004 S1 was subjected to both a short and long rejuvenation time retest, which accounts for the two numbers, with the long rejuvenation being the longer retest value.

This chapter covers the flat and folded test first. Each test is discussed, including details of testing errors and explanation of data variations. The flat and folded tests are then compared side by side. In order to draw conclusions from the fitting data, an attempt is made to model the data by fixing the relaxation times at a point where a majority of the tests still show high confidence fits. The final section discusses the results of the shape test.

Flat		Test	Retest
SN	**#**	**days**	**days**
001	A	1.6	1.9*
001	B	1.6	2.1*
001	C	1.9	2.6*
001	D	1.9	2.0*
001	E	2.0	2.2*
001	F	19.9	2.8*
001	G	6.0	3.1
001	H	6.0	3.1
001	I	6.0	3.1
001	J	13.0	
002	A	6.5	6.0
002	B	6.5	6.0
002	C	13.0	
003	A	6.5	6.0
003	B	13.0	
004	A	20.0	
004	B	9.0	
005	A	20.0	
005	B	9.0	
006	A	20.0	
006	B	9.0	

Folded		Test	Retest
SN	**#**	**days**	**days**
001	S1	5.9	
001	S2	4.9	4.2
002	S1	4.0	2.0
002	S2	7.0	
003	S1	2.8	1.2
003	S2	6.8	
004	S1	4.0	2.1 17.9*
004	S2	7.0	
005	S1	2.0	2.9
005	S2	7.0	
006	S1	2.0	7.0
006	S2	11.1	

Shape		Test
SN	**#**	**hrs**
001	L1	7.0
002	L1	12.0
002	L2	7.0
003	L1	7.0
004	L1	12.0
004	L2	7.0
005	L1	7.0
006	L1	7.0

*Represents retest performed several days after initial test

Table 2. Tests Performed

4.1 Flat Tests

Twenty-One flat tests were conducted for time lengths from less than two up to nearly twenty days. Fitting is accomplished in order to determine the relaxation time constants. The relaxation time constants of the initial tests determined the time of test required to accurately fit the stress relaxation. The first five flat test relaxation data were taken over a 38 hour period. The sixth flat test, performed on sample SN001 F with a duration of 478 hours. The results of the initial flat tests show a relaxation time between approximately 5 and 142 hours for virgin specimens. A test to accurately measure relaxation time is required to be five times the relaxation time, using a guideline from control theory. To reach five times the relaxation time requires a test time period between 25 and 710 hours. Time constraints prohibited the 30 day tests necessary to reach 710 hours, so further flat tests were performed for the maximum time available of between 144 to 480 hours. These tests were conducted using samples taken from each tape spring as well as several more from SN 001. Figure 18 shows select flat test results along with the fitting data plotted as the solid red lines. The shortest curve shown, SN001 A, demonstrates the inability of the shorter initial tests to accurately capture the secondary region's relaxation time. The values obtained from the fitting of select flat test results are shown in Table 3 with primary region relaxation time (t1) and secondary region relaxation time (t2). The relaxation times are calculated by taking the MATLAB fitting results and reversing from Equation 4 to Equation 3 to solve for (η/E). The value of (η/E) for the first and second exponential terms represents t1 and t2 respectively. The columns in Table 3 marked with a 'R' represent fits obtained from redistributed data. The r^2 terms are the coefficients of determination for the fit.

Figures 19 and 20 show the fitting calculated for the flat test of SN 001 A. A redistribution was performed to more heavily weight any fitting performed to that portion

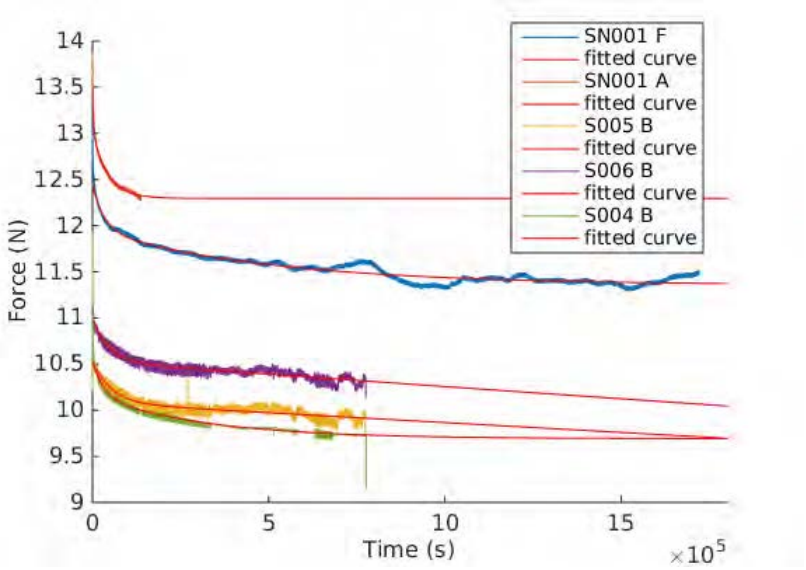

Figure 18. Select Flat Tests

Sensor	**SN**	**#**	r^2	r^2 **R**	**t1**	**t1 R**	**t2**	**t2 R**
NANO 43	001	A	**0.997**	0.997	**1.0**	0.2	**12.3**	6.7
NANO 43	001	F	**0.965**	0.993	**9.9**	0.2	**142.2**	5.1
NANO 43	004	B	**0.987**	0.996	**8.7**	3.8	**89.4**	57.5
LGP 312	005	B	**0.895**	0.999	**14.2**	0.5	**23695.5**	20.4
LGP 312	006	B	**0.921**	0.965	**13.1**	14.3	**10052.0**	2068.0

Table 3. Select Flat Test Fitting Results of Original and Redistributed Data

of the data with the greatest time dependence, the primary relaxation region. The redistribution is accomplished by adjusting the time points to a log scale distribution and then interpolating the values for these time points. Fitting is performed utilizing Equation 4 represented by the solid lines. The vertical lines show the 98% steady state condition for the first and second term in Equation 4. Table 3 compares the fits obtained from redistributed data to the original data for select tests. The bold values represent the fit obtained from the original data. The redistribution improves the fitting of the primary relaxation region but sacrifices the fitting of the secondary relaxation region. The fitting values obtained also show the variability of results. In some cases the redistributed data achieves a superior fit but in most cases the fits to the original data are best.

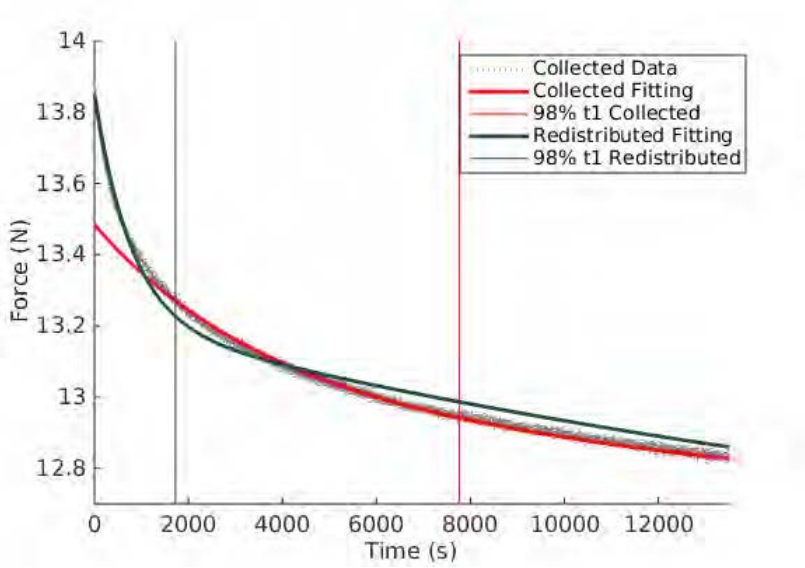

Figure 19. Collected and Redistributed Fitting Flat Test SN001 A Primary Relaxation

Along with Figures 19 and 20, later test data show the difficulties present in acquiring a satisfactory fit of the primary relaxation region even with the data redistribution. Figure 21 shows several fits attempted on redistributed data. The equation used for fitting is Equation 4 which is also shown on the figure. The fits attempted on the redistributed data display the primary culprit of poor fit: the fit functions inability to match the initial data. Two separate errors are shown in Figure 21. The first error, shown by SN 002 B, occurs when the fitting ignores or under-represents the initial data. The second error is caused by the method of test. The second error is induced by the initial load up period being different for each sample. The load up is different for each test since it is performed by hand on separate and slightly different test apparatuses. When the load up is quick and clean the results are similar to those shown by SN 003 A with a near vertical initial slope. When the load up is slower or uneven the initial slope is much shallower as shown by SN 002 A. This error in initial reading can also be linked to the sensor sensitivity difference between the NANO 43 and LGP 312 sensors.

It was decided that fitting to the original data provided the best fit for the purposes

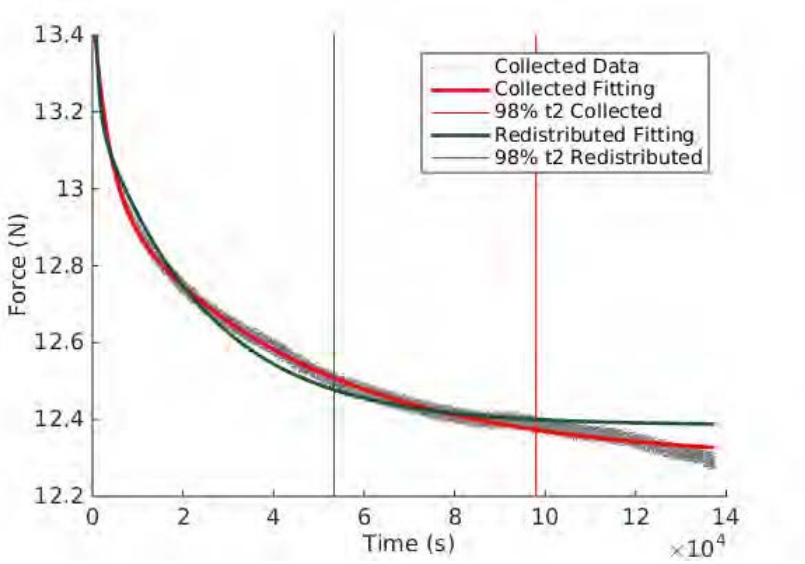

Figure 20. Collected and Redistributed Fitting Flat Test SN001 A Secondary Relaxation

of this thesis. Fitting original data ensures focus on the latter regions of the tests, which were most consistently recorded and most pertinent to long term relaxation. The inability to consistently capture the primary relaxation data means that only a few of the collected tests have sufficient data in that region to make accurate fits. There is also sufficient cause to question the credibility of the primary relaxation data even for those tests able to capture the primary region due to the inconsistent methods in load up.

Retests were performed on several samples to determine the effects of returning a sample to the as-manufactured shape on the level of internal stress. Two types of retests were used, the first type were performed several days after the end of the initial test. The second type of retests were performed sixty seconds after the conclusion of the initial test, allowing only sixty seconds of rejuvenation time. For the first type of retest, select initial tests are plotted next to their retest in Figure 22. The retest fitting results are shown as compared to the initial fitting results in Table 4. The first three rows show the first type of retest, performed on samples SN001 A, C, and

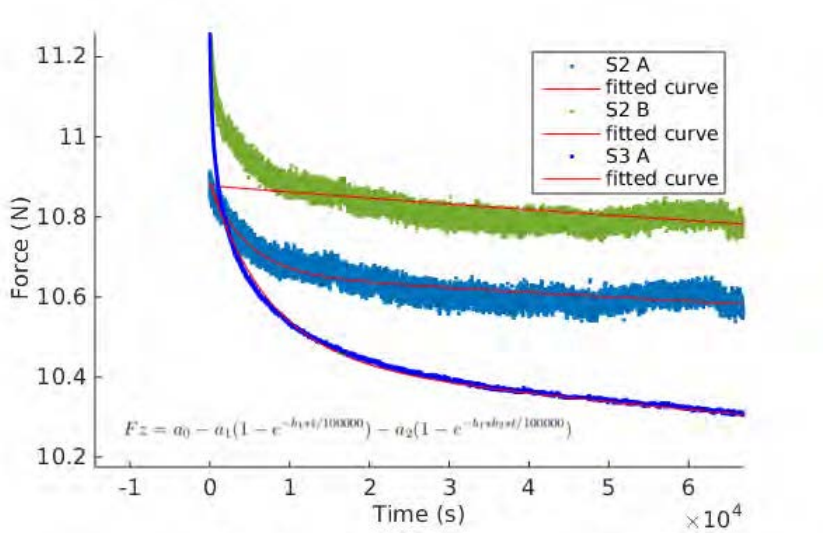

Figure 21. Common Fitting Errors

E. The first type of retests show a significant and consistent difference to the virgin runs.

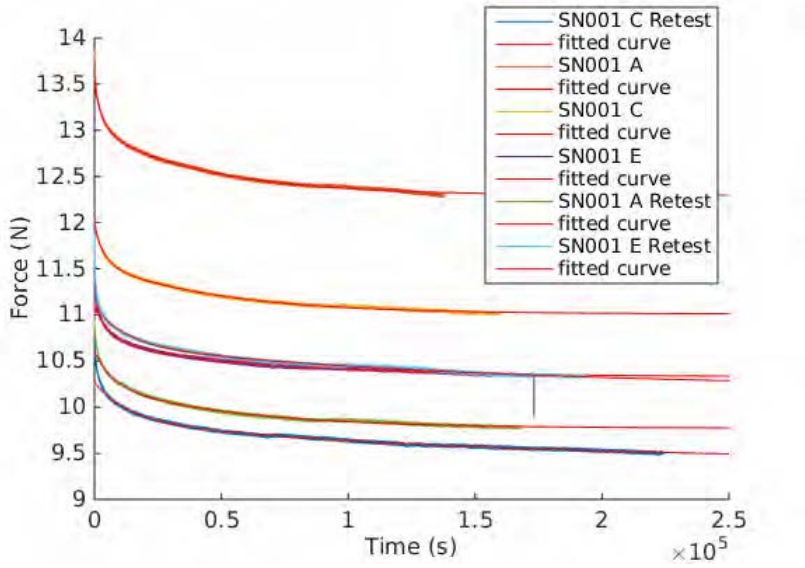

Figure 22. Flat Test Initial Data Compared to Long Rejuvenation Retest Data

Select short rejuvenation retest fits, the second type of retest, are also shown in Table 4 in the remaining three rows. Recall that these retests were performed by releasing the samples for only one minute and then reloading. However, Table 4 shows the difficulty in consistently fitting these data. The common errors mentioned

above are the primary cause of the poor fitting results. The fits performed on the LGP 312 data are especially poor with the second exponential term in Equation 4 dropped from the fitting causing an infinite secondary region relaxation time.

			Test			**Retest**		
Sensor	**SN**	**#**	r^2	**t1**	**t2**	r^2	**t1**	**t2**
NANO 43	001	A	0.997	1.0	12.3	0.995	2.0	14.5
NANO 43	001	C	0.997	0.9	11.7	0.996	3.6	36.8
NANO 43	001	E	0.995	1.1	11.7	0.9947	3.4	39.8
NANO 43	003	A	0.980	2.1	52.2	0.933	2.8	14118.9
LGP 312	002	A	0.959	86.1	INF	0.542	12.0	INF
LGP 312	002	B	0.965	82.8	INF	0.469	10.6	INF

Table 4. Flat Test Initial Fitting Data Compared to Retest Fitting

During conduct of the flat tests, several potential sources of error were noted that are not as easily described from the resulting plots. Friction on points of the tape spring in contact with the testing apparatus could provide a force that has not been accounted for. The load placed on the tape spring by the LGP 312 sensors is different than the load placed by the NANO 43 sensor. The temperature effects on the sensor are accounted for, but not the effects of temperature on the sample itself. The effects of humidity are also not accounted for. Some consideration must also be given to the order of the tests. The samples tested initially aged less than the samples tested later and raise the question: was this aging a significant factor? Finally, as Struik mentions, the time since the tape spring was last at or above its glass transition temperature effects how it ages [25]. Since the tests were conducted months after the sample creation, all the tests fall into short term creep behavior.

It should also be noted, the flat tests were performed under a variety of test conditions. Three separate sensors were used. Each sensor used a different apparatus, albeit of the same design, to secure the tape spring to the sensor. Also, the flat test was conducted in two different lab spaces. All these differences add to the complexity of discovering the root cause of some of the minor test variances.

4.2 Folded Tests

Folded tests were performed on samples taken from each tape spring for time periods ranging from 48 to 144 hours. The results of select folded tests are shown in Figure 23. Similar to the flat tests, data fitting is attempted in order to determine relaxation time. The fitting results are shown as the solid red lines in Figure 23. The results from these initial folded tests show a relaxation time between approximately 3 to 12 hours. Later tests, were performed on various samples for a minimum of the 60 hours needed to accurately capture the relaxation time. The 60 hours is again based on the guideline from control theory of five times the relaxation time. The fitting data obtained is shown in Table 5.

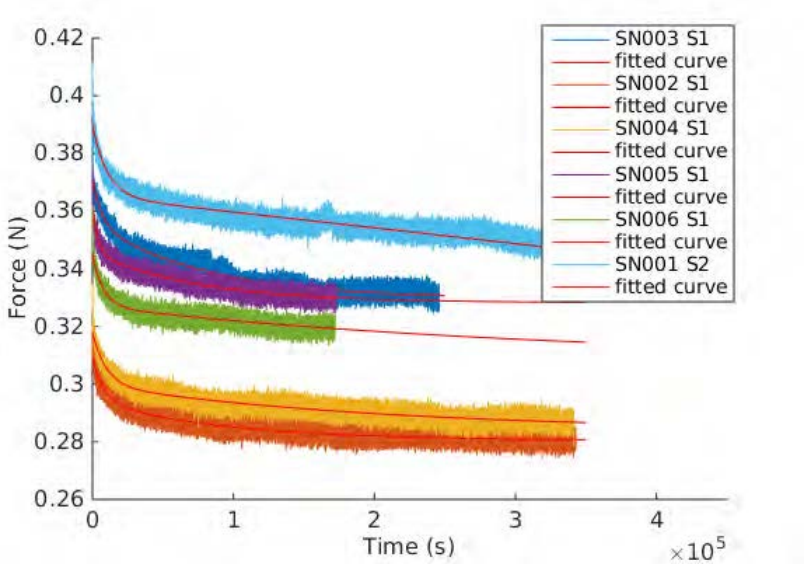

Figure 23. Select Folded Test Results

The initial folded tests were also subject to a quick rejuvenation attempt as discussed in Chapter III. Figure 24 shows the quick rejuvenation test run on sample SN006 S1. The measurement of the stress relaxation behavior after this rejuvenation is shown as the short rejuvenation data in Table 5. The folded retests were performed similarly to the flat secondary tests with a release from test of one minute

Short Rejuvenation

		Test			Retest		
SN	**#**	r^2	**t1**	**t2**	r^2	**t1**	**t2**
003	1	0.927	1.7	22.5	0.500	2.0	175.2
002	1	0.842	2.2	25.7	0.724	0.1	12.4
004	1	0.860	2.7	57.1	0.616	1.3	6497.5
005	1	0.881	1.0	21.1	0.659	1.7	565.2
006	1	0.826	2.1	89.9	0.765	2.5	2477.4
001	2	0.913	2.9	7281.3	0.649	0.8	32.9

Long Rejuvenation

		Test			Retest		
SN	**#**	r^2	**t1**	**t2**	r^2	**t1**	**t2**
004	1	0.860	2.7	57.1	0.886	1.7	107.3

Table 5. Select Folded Test Fitting Results

and then subsequent reloading. Figure 25 shows the initial and final force level from the test on a virgin sample, compared with the initial and final force value of the rejuvenation test. From the folded to the initial values an immediate rejuvenation of 6.6% is obtained. The retests were not performed sufficiently long for enough tests to accurately determine the relaxation time. Evidence of the inadequate test length can be seen by the poor r^2 values in Table 5; however, the results appear to show that after rejuvenation the tape springs secondary time constant may be extended. At the bottom of Table 5 is the long rejuvenation retest of SN004 S1. This test is the only folded test performed utilizing the same method as the flat test long rejuvenation retests with a rejuvenation period of several days.

Similar to the flat test, there are several areas that have potential to induce errors. The first area is the precise location of the sample with respect to the wind tunnel balance. The sample was placed at the same distance on the balance utilizing a tape measure to determine location. This measurement could get the sample close, but a better fixture could be designed so the sample would always contact in the same spot. The sample could also have a slight twist induced because the ends were not forced to end up in the same spot each test. The effects of temperature and humidity are

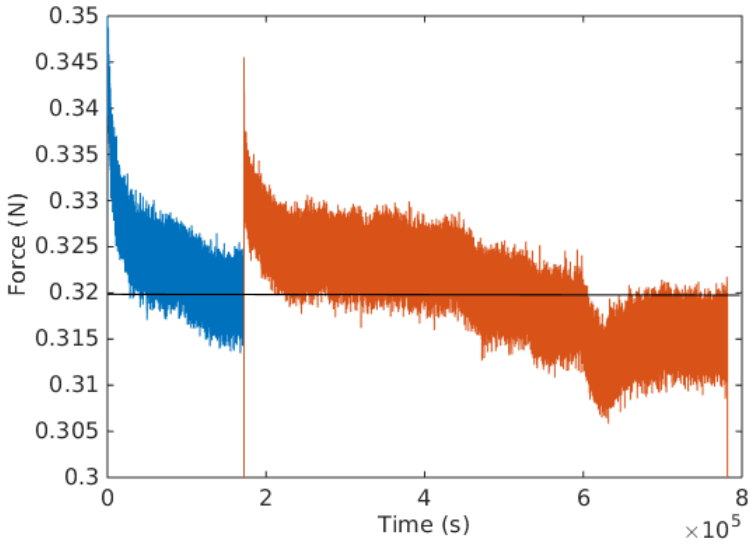

Figure 24. Folded Test with Rejuvenation

also of concern, primarily on the sample itself. All of the folded tests were performed on the same apparatus, utilizing the same sensor, and being performed in the same lab space.

4.3 Comparison of Flat and Folded Tests

Both the flat and folded tests are intended to capture the stress relaxation in a tape spring that is similar to the stress relaxation of a rolled tape spring. Since both tests have the same intention their results should be similar. Figure 26 shows a comparison of a flat test with a folded test. Since each test measures at a different level of force, the relaxation is shown as a percentage of the original force level. The figure clearly shows that both tests are in excellent agreement. Both tests result in 85% of the initial stress level remaining after 10 days of testing.

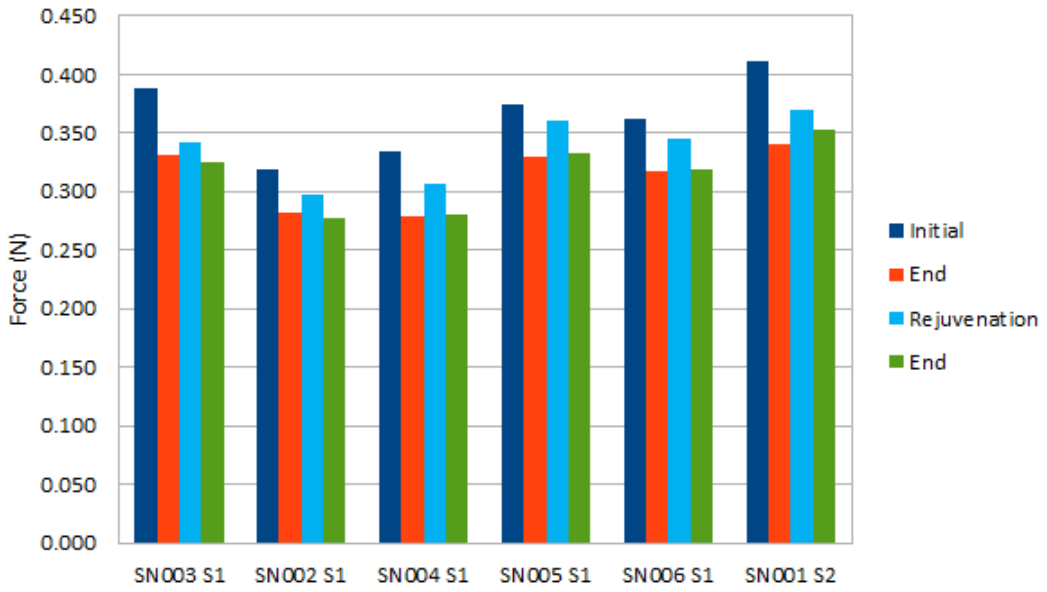

Figure 25. Immediate Rejuvenation Results for Folded Tests

4.4 Modeling

A model is created for the flat and folded tests in order to draw conclusions from the data. The model is created by determining the relaxation times t1 and t2 that fit a majority of the tests with high r^2. The results of the flat tests and folded tests are consistent within a reasonable means. Modeling is necessary due to the inconsistent fitting achieved using MATLAB's standard 'fit' function. For the initial flat tests, the shorter test on samples A to E do not provide sufficient length to determining the secondary region's relaxation time constant. The results of Flat Test F show that the secondary relaxation time may be closer to the hundreds of hours versus the tens of hours shown by the shorter tests. When reviewing the results of Flat Test F closely, the fit is very poor in the initial period due to the majority of the data being in the latter parts of the test. Figure 27 shows MATLAB fitting of several flat and folded tests. In order to show these tests overlaid, the force is normalized as a percentage of the force at roughly thirty hours into the test. Normalizing to this later force is ideal

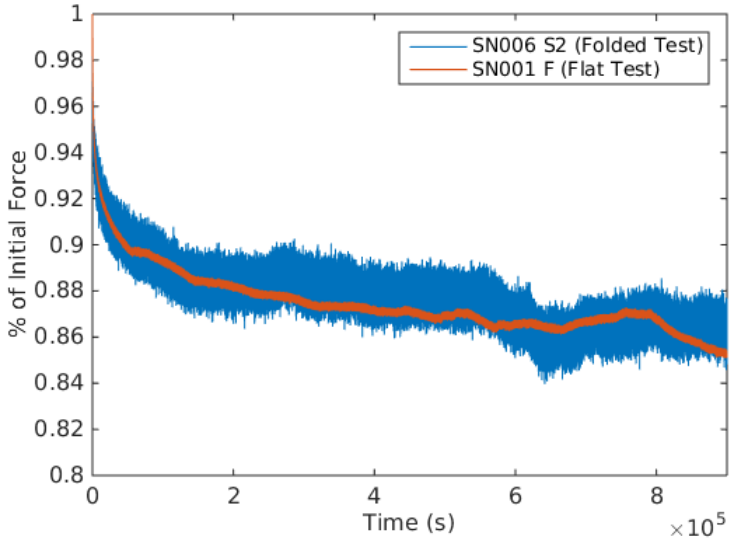

Figure 26. Flat Test Results Compared to Folded Test Results

because the latter parts of the test are consistent, but the initial portions of the test differ due to differing initial load-ups of the samples. The fit most off center is SN001 A, again due to the length of test being too short for accurate measurements. The fit showing the longest relaxation time constant is from the test SN006 S2. This fit has a relatively low r^2 of 0.82, as does the other folded test primarily due to the noise level of these data. Figures 28 and 29 show the confidence bounds of the fit results.

Several attempts were made to find a set of relaxation constants that fit both folded and flat tests of various testing lengths. Demonstrations of the quality of the final fixed relaxation time constants are shown in Figure 30. The result is the most likely relaxation times of t1 of 1.4 hours and t2 of 92.6 hours. Reviewing the remaining tests show that this relaxation time combination provides a good fit for all flat and folded tests performed. The model demonstrates the similarity of the data despite the inconstant fitting results utilizing MATLAB. The fit of SN001 A again presents a poor relation with the other tests due to its limited length. The average r^2 values of fits with the fixed t1 and t2 are shown in Figure 31. An educated guess had to be made for the value of t1 because the test data is inconsistent during this

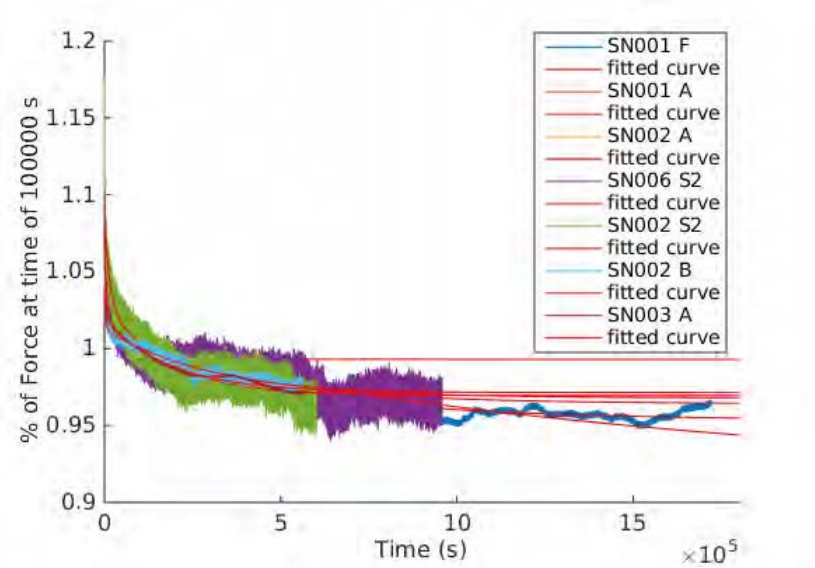

Figure 27. Modeled Fitting Results

initial period. The t1 value is fixed at 1.39 hours and the value of t2 varied to find the value that achieves the best fit for the various tests. The 'Free' r^2 shown in Figure 31 represents the average r^2 of fits obtained using the various t1 and t2 values as determined by MATLAB's 'fit' command.

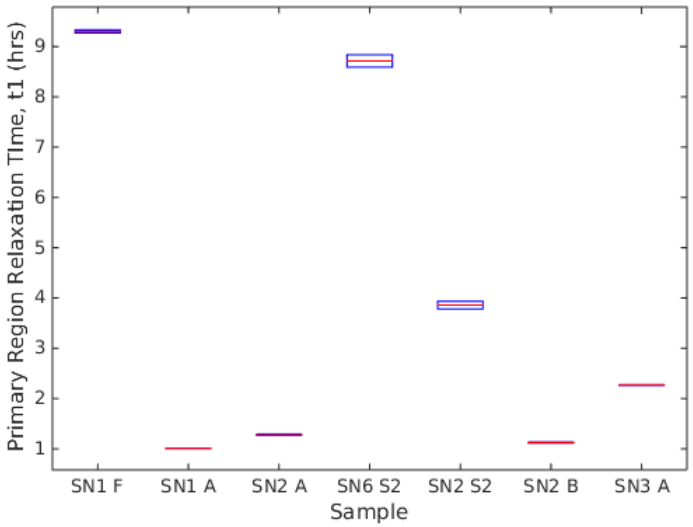

Figure 28. Primary Region Relaxation Times for Select Samples

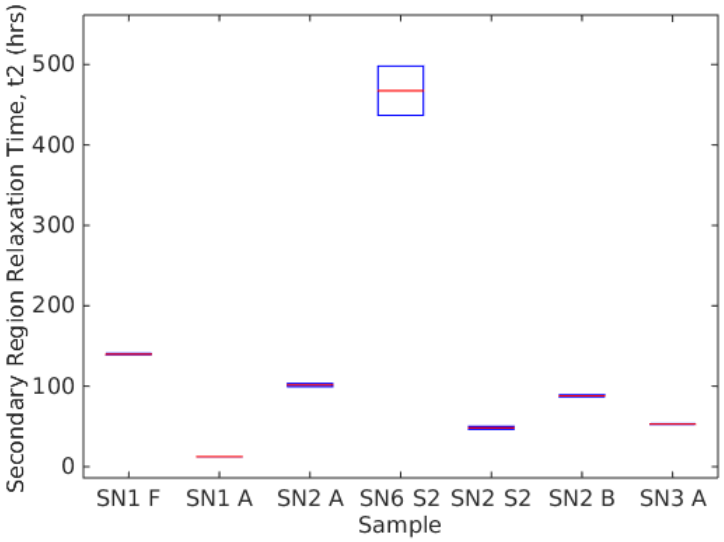

Figure 29. Secondary Region Relaxation Times for Select Samples

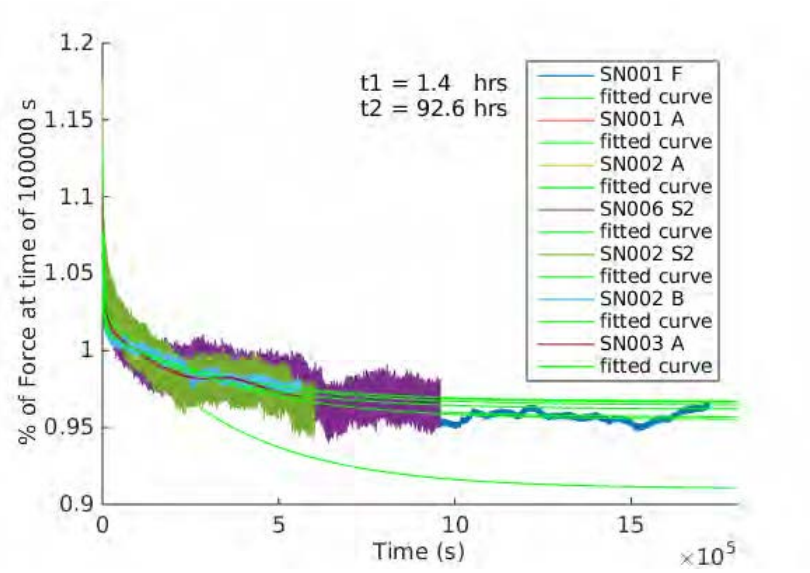

Figure 30. Modeled Fitting Results

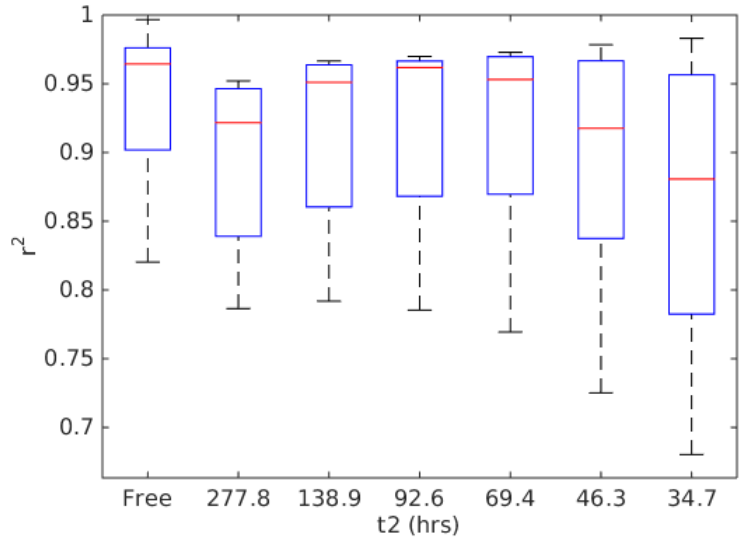

Figure 31. Fitting Values with Fixed Relaxation Times

4.5 Shape Tests

Shape tests were performed initially on two samples at expanding intervals of 1 hr, 2 hrs, 4 hrs, 19 hrs, 67 hrs, 90 hrs, 115 hrs, and 281 hours. The folded and flat test showed primary region relaxation times less than 5 hours, so a second test was conducted for six samples (one from each tape spring) that scanned the tape spring at the shorter initial intervals called out in Chapter III. The results of these tests on the measurements taken from S004 are shown as overlaid SolidWorks models displayed in Figure 32.

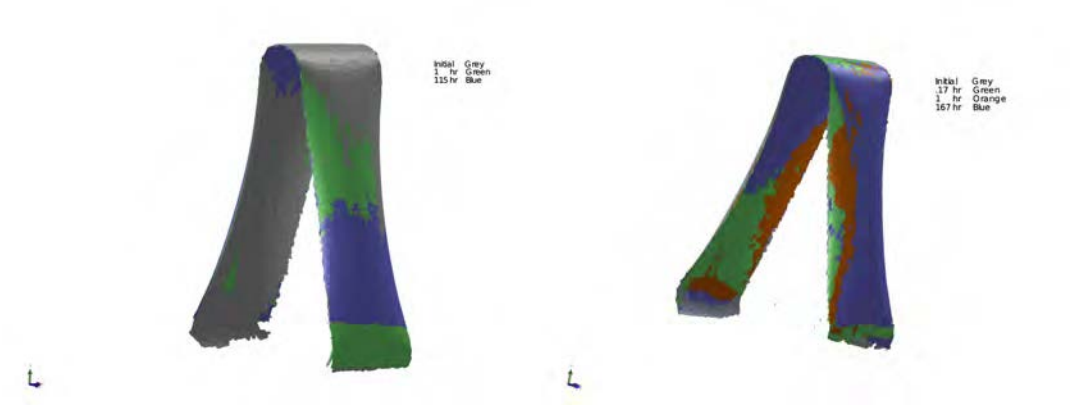

Figure 32. S004 Shape Tests

In order to create useful data from these shape tests, cross sections were taken at intervals along the face. The cross sections were created in PolyWorks by taking a set of cross sections over a user defined curve that wrapped over the face and top of the tape spring samples. The results at three sections for sample S004 are shown in Figure 33. The cross sections are then analyzed utilizing a Taubin method fitting function for an ellipse. The fits are solved in the form of the generalized equation and must be converted to the implicit equation to enable comparison of the calculated radii of the ellipse. The implicit data results are shown in Figure 34 and 35.

In Figure 34 each line represents the minor axis radii for each cross section over the duration of the test. The lower the radius of the minor axis the closer the cross

section is to the flat section at the top of the tape spring. The cross sections for the portion of the tape spring too flat for a reasonable ellipse fit were dropped from the plot. Figure 35 shows the fitted slope of the minor axis radii over the course of the test. When the value is below zero, the minor axis radii decreases over the duration of the test and thus the section flattens out. When the value is above zero, the minor axis radii increases over the duration of the test and thus the tape spring becomes more curved. Notice in the figure that the slope is in millimeters per hour and the greatest rate measured is 0.00002. Upon review of Figure 34, the noise in measurements is greater than the slope measured.

Potential areas for error discovered while testing include many of the same as discussed for the flat and folded test. The samples are difficult to load and measure at equal intervals on the test apparatus as designed. Temperature and humidity effects are not accounted for. The 3D images in Figure 32 show that there is a visible amount of motion in the location of the top fold. The motion presents itself as a change in the 'lean' of the sample. Lean meaning a motion of the top fold toward on of the constraining folds. The motion should not effect the measurement of the ellipse radius since the ellipse fit is invariant to the location of the shape.

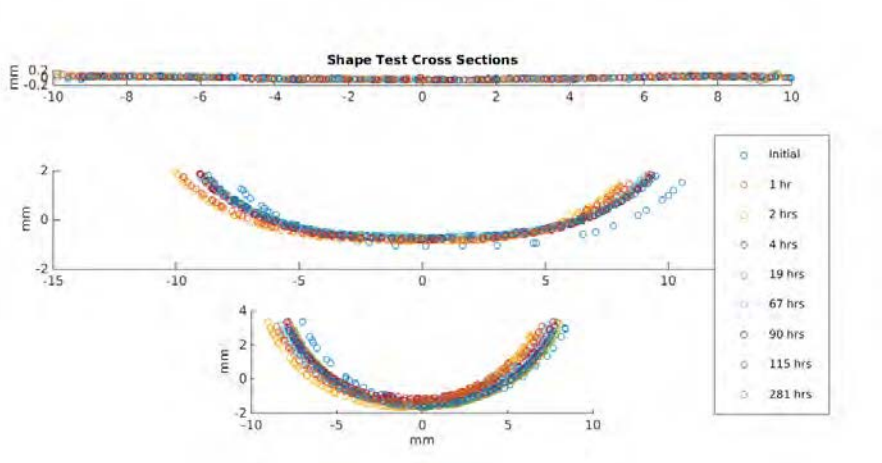

Figure 33. Cross Sections

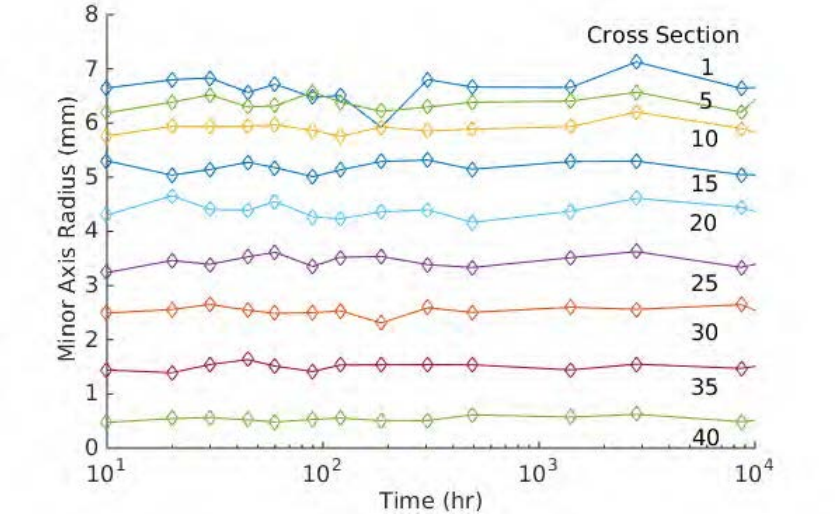

Figure 34. Shape Data Minor Axis Radii

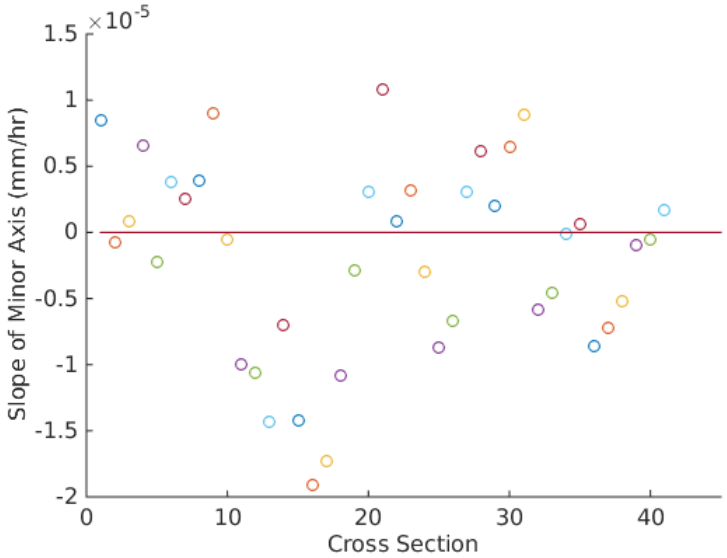

Figure 35. Shape Data Minor Axis Change in Radii

4.6 Summary

The results of the tests performed for this thesis have been presented. Data have been collected from the three test configurations: flat, folded, and shape. Forty-one tests were conducted in an exploratory fashion into the breadth of tests possible for the three configurations. The data are shown and fitting performed in order to determine patterns in the behavior. Conclusions based on these data, including confidence and limitations are presented in Chapter V. The test methods showed room for improvement, recommendations for these improvements are also made in Chapter V.

V. Conclusions

Considering the preceding data, the following conclusions have become apparent. Data on stress relaxation have been collected utilizing two unique methods, three types of sensors and over a variety of lengths of time. Fitting the data presented a challenge; however, using simple stress analysis techniques a good fit was obtained for the flat and folded tests setups. The shape test proved relatively simple to conduct and analyze. The results of this test did not show any effects that could be attributed to or correlated with stress relaxation. One of two conclusions can be drawn from the lack of any variation of the shape. The first conclusion is that the test was unable to capture the changes in shape. The second, and more likely, conclusion is that there is no change in the shape over time. The implication of the second conclusion is that any stress relaxation occurring is caused by internal changes and these changes do not modify the shape of the tape spring.

So to answer the first question of this thesis: *Are there methods of imitating the rolled configuration in which changes in internal stress can be measured via stress relaxation?* Yes, the results of the flat and folded tests show stress relaxation. The fact that these results are consistent between the tests shows that the major trend in relaxation is being captured. To answer the second question: *Is the behavior consistent and reasonable?* Yes, the behavior is consistent, but test methodology and analysis could be improved for more consistent fitting. The third question proved to be beyond the scope of this thesis: *What is the effect of temperature?* What is apparent from the results is that temperature has a significant effect, which is consistent with theory and experimental results [6, 8, 9, 12, 13, 14, 22, 25, 26, 27]. The final question provided a promising answer: *What is the effect of allowing the tape spring to return to its extended form after a period of deformation?* From the tests conducted, there appeared to be a significant recovery of internal stress by simply

unfolding or releasing compression from the tape spring.

5.1 Confidence in the Data

The data fitting did not produce consistent results without forcing t1 and t2 values as performed in the Section 4.4. The inability to fit was caused by several factors that included the test methodology, the equation used, and corresponding methods of obtaining a fit to the data. These factors must be addressed to increase the robustness of the tests presented.

Several recommendations are presented to improve the flat test methodology. The first recommendation is the creation of a test apparatus that applies the load at the beginning of the test in a measurable and controllable strain rate. The second recommendation is the performance of the test in a temperature and humidity controlled chamber to eliminate the fluctuations in these factors. The final recommendation is a new fixture that applies the compression on the tape spring sample without the potential of friction forces. The fixture might involve the use of roller bearings at the contact points to distribute the load uni-axially.

Several recommendations are presented to improve the folded test methodology. Similar to the flat test, both a climate controlled chamber and modification of the test fixtures are recommended. For the folded test an improved fixture would provide positive control at the ends of the folded spring, ensuring consistent shape of the folded samples. Again, loading is critical to understanding the primary relaxation region, so an improved loading apparatus is desirable. This apparatus would ideally be able to control and output the strain rate during the loading.

To improve the fitting results, it is recommended that the equation used be revisited and new fitting methods be explored. The equation used in this thesis had difficulties capturing the transition region between the primary and secondary re-

laxation regions, this may be improved by adding a third exponential term to the equation. The fitting method used was MATLAB's fitting function with the custom equation being Equation 4. A more robust method of fitting specifically designed for relaxation or creep behavior could improve results [7, 15, 23].

The relaxation results produced by both the flat and folded relaxation tests provide consistent results. The result, as presented in Chapter IV, is that the initial region relaxation time (t1) is modeled to be around 1.4 hours, and the secondary region relaxation time (t2) is modeled to be on the order of 92.6 hours. Utilizing Equation 4 with these time constants achieves a good fit to all the measured data. Further testing utilizing methods incorporating the recommendations above is necessary to achieve more precise relaxation time constants.

Along with the relaxation times, the secondary tests and retests performed on select samples also provide insight into the ability of the tape springs to be rejuvenated prior to launch. A recovery of roughly six percent of the initial stress from the relaxed stress value is calculated. This result shows that recovery of the internal stress level is possible by simply allowing the tape spring to return to its as manufactured form. The level of this recovery requires further testing to achieve confidence in the specific value.

The shape tests were likewise consistent in their results. The shape test did not provide significant results, except the lack of change in shape. Since the shape tests did not show signs useful to determine the aging of a rolled tape spring, it is not a recommended test for this purpose. Another method that may achieve useful results would be to measure the change in shape of a flat test sample before and after its compression test. The samples used in this thesis showed a significant (visible) change in shape from before and after the test. This change in shape could be measured and used to provide additional insight into the tape spring aging.

5.2 Limitations and Future Work

As mentioned in Chapter III, a sufficient number of tests were not conducted in this thesis that are required in order to determine several important aging properties. The first aging property being the determination of long term creep, which is quite different from short term creep, as discussed by Struik [25]. In order to obtain this data, use of the time-temperature superposition principle is required. The time-temperature superposition principle requires creep (or relaxation) tests be performed at several temperatures so that this temperature dependence can be completely characterized. This characterization leads to the creation of a 'master curve' from which the physical aging of samples can be determined with aging times much greater than testing times. The relaxation times found in this thesis simply provide a short term relaxation curve general profile. In order to appropriately extrapolate physical aging effects temperature tests are required.

A second limitation of this work is that it is impossible to say that the measured behavior is exactly what happens to a tape spring in a rolled configuration. In order to correlate these two the following work is recommended. First, increased understanding of the relaxation behavior is required utilizing improved test methods and the time-temperature superposition principle. Once this data is collected, a model should be constructed to predict the expected behavior of a rolled tape spring over time. To test this model, deployment tests should be conducted on rolled tape springs of various ages. The correlation of the deployment tests and the model will demonstrate if the stress relaxation tests fully and accurately capture the aging of rolled tape springs.

Future work is also recommended to better understand the rejuvenation methods possible. It is believed, based on the research presented in Chapter II, that rejuvenation may be possible by elevating the temperature of the sample above its glass

transition temperature T_g. It may also be possible to achieve this recovery at an elevated temperature that remains under T_g. To perform this study, several samples would be required to be aged and then rejuvenation attempted via various means. In order to confirm the results, deployment tests of aged and rejuvenated samples would likely be required.

5.3 Summary

With the results obtained in this thesis, confidence can be given to the flat and folded methods of measuring stress relaxation. Based on the results of the tests performed, the secondary region relaxation time of a rolled tape spring at room temperature is on the order of 100 hours. Rejuvenation via temporary release from strain is a promising means of reducing the impact of loss in stiffness. Shape testing was insufficiently accurate to capture any changes in shape. Additional testing and analysis is required to fully characterize the relaxation behavior of a rolled tape spring. The methods presented provide a simple means of collecting stress relaxation data at various temperatures over long periods of time. The samples required are limited and the sensors simple, providing the opportunity to test many samples cheaply. These test methods can be scaled to accommodate much larger sample sizes. Several means are now available to measure the internal behavior of a rolled tape spring.

Bibliography

1. Adams, Douglas and Mobrem, Mehran. "Lenticular Jointed Antenna Deployment Anomaly and Resolution Onboard the Mars Express Spacecraft." *Journal of Spacecraft and Rockets* 46.2: 403-410 (2009).

2. Bayram, Y. et. al. "E-Textile Conductors and Polymer Composites for Conformal Lightweight Antennas." *IEEE Transactions of Antennas and Propagation* 58.8: 2732-2736 (2010).

3. Campbell, Flake C. *Manufacturing Processes for Advanced Composites*. New York: Elsevier, 2004.

4. Chawla, Krishan K. *Composite Materials Science and Engineering*. New York: Springer, 2013.

5. Cool, Grant R. *Atomic Oxygen Erosion Resistance of Organic Polymers for Low Earth Orbit Spacecraft*. PhD dissertation. University of Toronto, Toronto, Canada, 1996 (0-612-35431-8).

6. Gates, Thomas S. and Grayson, Michael A. "On the Use of Accelerated Aging Methods for Screening High Temperature Polymeric Composite Materials." *40TH Structures, Structural Dynamics, and Materials Conference and Exhibit* 925-935 (1999).

7. Haj-Ali, Rami M. and Muliana, Anastasia H. "A multi-scale constitutive formulation for the nonlinear viscoelastic analysis of laminated composite materials and structures." *International Journal of Solids and Structures* 41.13: 3461-3490 (2004).

8. Hodge, Ian M. "Physical Aging in Polymer Glasses," *SCIENCE* 267: 1945-1947 (1995).

9. Iqbal, K. and Pellegrino S. "Bi-Stable Composite Shells." *41st AIAA/ASME/ASCE/AHS/ASC Structures, Structural Dynamics and Materials Conference* (2000).

10. Jennings, Alan, Black, Jonathan and Gutierrez, Alyssa N. "Geometry and Moments of Bent Tape Springs." *54th AIAA/ASME/ASCE/AHS/ASC Structures, Structural Dynamics and Materials Conference* (2013).

11. Kaya, Deniz. "Polymer Properties and Deformations." Date Retrieved: 22 Aug 2014. http://www.denizkaya.net/plastik-muhendisligi/polymer-properties-deformations/.

12. Kwok, Kawai and Pellegrino, Sergio. "Viscoelastic Effects in Tape-Springs." *52nd AIAA/ASME/ASCE/AHS/ASC Structures, Structural Dynamics and Materials Conference* (2011).

13. Kwok, Kawai and Pellegrino, Sergio. "Folding, Stowage, and Deployment of Viscoelastic Tape Springs." *AIAA Journal* 51.8:1908-1918 (2013).

14. Makuch, Alessa J., and Reynolds, Whitney D. "In Situ Measurements of Viscoelastic Effects in Composite Tape Springs." *SPIE Smart Structures and Materials+ Nondestructive Evaluation and Health Monitoring.* International Society for Optics and Photonics (2012).

15. Muliana, Anastasia H. and Kim, Jeong Sik. "A concurrent micromechanical model for predicting nonlinear viscoelastic responses of composites reinforced with solid spherical particles." *International Journal of Solids and Structures* 44.21: 6891-6913 (2007).

16. United States/Department of Defense.
MIL-HDBK-17-1F Composites Materials Handbook. *Volume 1. Polymer Matrix Composites Guidelines for Characterization of Structural Materials*. 17 June 2002.

17. Mobrem, Mehran and Adams, Douglas. "Deployment Analysis of Lenticular Jointed Antennas Onboard the Mars Express Spacecraft." *Journal of Spacecraft and Rocets* 46.2: 394-402 (2009).

18. Murphey, Thomas. "Large Strain Composite Materials in Deployable Space Structures." *17th International Conference on Composite Materials* (2009).

19. Patz Materials and Technologies. 4968 Industrial Way Benicia, CA http://patzmandt.com/

20. Peterson, Michael. *High Shear Strain Characterization of Plain Weave Fiber Reinforced Lamina*. Thesis. The University of New Mexico, Albuquerque, New Mexico, 2014.

21. Reynolds, Whitney. "Viscoelastic Behavior of the VPM Antennas." AFRL/RVSV, (3 July 2013). Unpublished.

22. Reynolds, Whitney. "Influence of Temperature on Deployment of Viscoelastic Composite Tape Spring Antennas." AFRL/RVSV. Unpublished.

23. Rudra, R. P. "A Curve-Fitting Program to Stress Relaxation Data." *Canadian Agricultural Engineering* 29:209-211 (1987).

24. Shames, Irving H. and Cozzarelli, Francis A. *Elastic and Inelastic Stress Analysis*. Philadelphia: Taylor & Francis Ltd, 1997.

25. Struik, Leendert C.E. *Physical Aging in Amorphous Polymers and other Materials*. New York: Elsevier, 1978.

26. Sullivan, J. L., Blais, E. J. and Houston, D. "Physical Aginging in the Creep Behavior of Thermosetting and Thermoplastic Composites." *Composites Science and Technology* 47: 389-403 (1993).

27. Sullivan, J. L. "Creep and Physical Aging of Composites." *Composites Science and Technology* 39: 207-232 (1990).

28. White, Jim R. "Polymer Ageing: Physics, Chemistry or Engineering? Time to Reflect." *Comptes Rendus Chimie 9* 11: 1396-1408 (2006).

Appendix A

```
%Tape Sping Thesis v5
%Created by: Justin Heppe
%Last Updated: 17 Feb 2015

%close all;clear all

%%
%Select file(s) desired to analyze
num=[]; %input array of test numbers desired
%20g demo 56(1) 29
%100g demo 2 56(3)
%Variable weight 54 55 56
%VACE Tests 32 34 36 40 42 44 46
%VACE Later Tests 47 69 71 72 73
%ATI Initial 16 17 18 19 20 21
%ATI Retest 23 24 25 26 27 28
%Later Flat Tests 63 66 67 68

%%
%Pull filenames from test numbers
[ files, freq, Source ] = filenames( num );

%%
%Parse data from differing file types
[ T1, T2, Fz, t ] = parse( files, freq, Source );
%Data is returned in cell format with the columns
%of the cell pertaining to the test number

%%
%Correct for Temperature
[ Fz ] = Temperature( T1,T2,Fz,t,Source );
 %Fz{1,2}=Fz{1,2}-Fz{1,2}(1);
 %Fz{2,2}=Fz{2,2}-Fz{2,2}(1);

%%
%Crop unnecessary and bad portions of data
[ T1,T2,Fz,t ] = crop( T1,T2,Fz,t );

%%
%Reduce number of data points for easier plotting
N=4000;
t1=t;
T11=T1;
T21=T2;
[ t,Fz,T1,T2 ] = reducer( t,Fz,T1,T2,N );

%%
```

```
%Plot Data
[h,q]=plotcell( T1, T2, Fz, t);

%%
%Log Log Plot
[h,q]=plotcell( T1, T2, Fz, t);
set(h,'xscale','log')
set(h,'yscale','log')
set(q,'xscale','log')
set(q,'yscale','log')

%%
%Redistribute points
[ FzR,tR ] = redistribute( Fz,t );

%%
%Fit data
[a, b, ci] = StressFittingUnknown(t,Fz);

%%
%Plot model lines
[c,d] = StressFittingForced(t,Fz);

%%
%Linear fit to loglog data
Fzlog=cellfun(@log,Fz,'UniformOutput',0);
tlog=cellfun(@log,t,'UniformOutput',0);
[ e ] = StressFittingLog( t, Fz, tlog, Fzlog );
```

```
function [ files, Freqs, Sources ] = filenames( num )
%Takes input test number and returns string of file name
%   Created by Justin Heppe
%   Last update: 17 Feb 2015

%%
%Must input all file names for the code to draw upon
tests={'./SensorCreep/RAW/20140823_250GDeadWeight_10MinuteWarmup_10Hz.txt'; %1
'./SensorCreep/RAW/20140825_100GDeadWeight_10MinutesWarmup_10Hz.txt';    %2
'./SensorCreep/RAW/20140827_50GDeadWeight_10MinutesWarmup_10Hz.txt';     %3
'./SensorCreep/RAW/20140828_50GDeadWeight_10MinutesWarmup_10Hz.txt';     %4
'./SensorCreep/RAW/20140903_24NDeadWeight_5Hz.txt'; %5
'./SensorCreep/RAW/20140915_24NDeadWeight_1Hz.txt'; %6
'./FirstTry_20140522/RAW/Fold_20140522_v0.txt';      %7
'./FirstTry_20140522/RAW/Fold_20140522_v0(0).txt';   %8
'./FirstTry_20140522/RAW/Fold_20140522_v0(1).txt';   %9
'./FirstTry_20140522/RAW/Fold_20140522_v0(2).txt';   %10
'./FirstTry_20140522/RAW/Fold_20140522_v0(3).txt';   %11
'./FirstTry_20140522/RAW/Tare_20140522_1.txt';       %12
'./FlatTest/RAW/20140820_FlatTestTrail1_10Hz.txt';   %13
'./FlatTest/RAW/20140829_FlatTestTrail2_1Hz_LongTerm.txt';
'./FlatTest/RAW/20140904_FlatTestTrial3_5Hz_Post24NPreLoad.txt'; %15
'./FlatTest/RAW/20140905_FlatTest_1A_1Hz_PostPreLoadandTrial3.txt';
'./FlatTest/RAW/20140906_FlatTest_1B_1Hz_Post1A.txt';
'./FlatTest/RAW/20140908_FlatTest_1C_1Hz_Post1B.txt';
'./FlatTest/RAW/20140916_FlatTest_1D_1Hz_PostPreLoad.txt';
'./FlatTest/RAW/20140918_FlatTest_1E_1Hz_Post1D.txt'; %20
'./FlatTest/RAW/20140924_FlatTest_1F_1Hz_Post20NPreLoad.txt';
'./FlatTest/RAW/20140924_FlatTest_1F_1Hz_Post20NPreLoad - Copy.txt';
'./FlatTest/RAW/20141014_FlatTest_1A_1Hz_Post1F_RETEST.txt';
'./FlatTest/RAW/20141016_FlatTest_1B_1Hz_Post1A_RETEST.txt';
'./FlatTest/RAW/20141018_FlatTest_1C_1Hz_Post1B_RETEST.txt';     %25
'./FlatTest/RAW/20141021_FlatTest_1D_1Hz_Post1C_RETEST.txt';
'./FlatTest/RAW/20141023_FlatTest_1E_1Hz_Post1D_RETEST.txt';
'./FlatTest/RAW/20141025_FlatTest_1F_1Hz_Post1E_RETEST.txt';
'./WithTemp_20141024/RAW/20141010_20GDeadWeight.txt';
'./WithTemp_20141024/RAW/20141014_20GDeadWeight_VariousTemps.txt';  %30
'./WithTemp_20141024/RAW/20141020_Removalof20G_CoolDown.txt';
'./Folded_Test/RAW/20141021_AdditionofPreSpringSample.txt';
'./Folded_Test/RAW/20141021_Tare_PreSpringSample.lvm';
'./Folded_Test/RAW/20141027_SN003S1_Folded_PostPreLoad.txt';
'./Folded_Test/RAW/20141027_Tare_SN003S1_Folded.lvm';            %35
'./Folded_Test/RAW/20141031_SN002S1_Folded.txt';
'./Folded_Test/RAW/20141031_SN003S1_Folded_PostSN003S1_AccidentShortTest.txt';
'./Folded_Test/RAW/20141031_Tare_SN002S1_Folded.lvm';
'./Folded_Test/RAW/20141031_Tare_SN003S1_Folded_AccidentalReload.lvm';
'./Folded_Test/RAW/20141106_SN004S1_Folded_PostSN002S1.txt';     %40
'./Folded_Test/RAW/20141106_Tare_SN004S1_Folded.lvm';
'./Folded_Test/RAW/20141112_SN005S1_Folded_PostSN004S1.txt';
'./Folded_Test/RAW/20141112_Tare_SN005S1.lvm';
'./Folded_Test/RAW/20141117_SN006S1_Folded_PostSN005S1.txt';
'./Folded_Test/RAW/20141117_Tare_SN006S1.lvm';           %45
```

```
'./Folded_Test/RAW/20141126_SN001S2_Folded_PostSN006S1.txt';
'./Folded_Test/RAW/20141205_SN003S2_Folded_PostSN001S2.txt';
'./Cooper_InitialTests/RAW/20141114_ATI_100G_1Hz_ConstantLoadTest';
'./Cooper_InitialTests/RAW/20141114_Cooper_100G_1Hz_ConstantLoadTest';
'./Cooper_InitialTests/RAW/20141117_ATI_50G_1Hz_ConstantLoadTest_PreHeated';
'./Cooper_InitialTests/RAW/20141117_Cooper_500G_1Hz_Constant ...
    LoadTest_PreHeated';
'./Cooper_InitialTests/RAW/20141119_ATI_100G_10Hz_ConstantLoadTest.txt';
'./Cooper_InitialTests/RAW/20141119_Cooper_100G_10Hz_Constant ...
    LoadTest_PreHeated.txt';
'./Cooper_InitialTests/RAW/20141121_ATI_Timed_VariableWeightTest';
'./Cooper_InitialTests/RAW/20141121_Cooper1_Timed_VariableWeightTest';
'./Cooper_InitialTests/RAW/20141121_Cooper2_Timed_VariableWeightTest';
'./Cooper_InitialTests/RAW/20141121_GARBAGE_DATA'; %57
'./Cooper_InitialTests/RAW/20141121_CombinedTest1';
'./Cooper_InitialTests/RAW/20141126_CombinedTest2';
'./Cooper_InitialTests/RAW/20141126_CombinedTest2_Continued'; %60
'./Cooper_InitialTests/RAW/20141202_CombinedTest3';
'./Cooper_InitialTests/RAW/20141202_CombinedTest3_Continued';
'./Cooper_InitialTests/RAW/20141202_CombinedTest4_C12A_C22B_A3A';
'./Cooper_InitialTests/RAW/20141212_CombinedTest5_C12A_C22B_A3A';
'./Cooper_InitialTests/RAW/20141229_CombinedTest6_C15A_C26A_A4A'; %65
'./Cooper_InitialTests/RAW/20150107_CombinedTest7_C15B_C26B_A4B';
'./Cooper_InitialTests/RAW/20150116_CombinedTest8_C11G_C22B_A3A';
'./Cooper_InitialTests/RAW/CombinedTest2.txt';
'./Folded_Test/RAW/20141212_SN005S2_Folded_PostSN003S2.txt';
'./Folded_Test/RAW/20141218_SN004S1_Folded_RETEST_PostSN005S2.txt'; %70
'./Folded_Test/RAW/20150105_SN006S2_Folded_PostSN004S1RETEST.txt';
'./Folded_Test/RAW/20150116_SN002S2_Folded_PostSN006S2.txt';
'./Folded_Test/RAW/20150123_SN004S2_Folded_PostSN002S2.txt';
};

%%
%For those tests where frequency was no recorded this provides
%the frequecy necessary to create the time array
[q,r]=size(tests);
freqs=ones(1,q);
freqs(1,1:15)=[10 10 10 10 5 1 1 1 1 1 1 1 10 1 5];

%%
%Create a list of sources so the parce function knows which source to
%assign to which file
sources=[1 1 1 1 1 1 2 2 2 2 2 2 1 1 1 1 1 1 1 1 1 1 1 1 1 1 1 2 2 ...
2 2 7 7 7 7 7 7 7 7 7 7 7 7 7 7 2 1 3 1 3 1 3 4 5 5 4 6 6 6 6 6 6 6 ...
6 6 6 6 2 2 2 2 2];

%%
%Finds the size of the number of tests desired
[m,n]=size(num);
i=1;

while i<=n
```

```
files{i}=tests{num(i)};
Freqs{i}=freqs(num(i));
Sources{i}=sources(num(i));
i=i+1;
end
end
```

```
function [ T1, T2, Fz, t ] = parse( files, freqs, Sources )
%Takes file name/location and parses data to provide RAW data (no
%filtering) in cell format
%   Created by Justin Heppe
%   Last update: 17 Feb 2015

%%
[m,n]=size(files);
i=1;

while i<=n
file=files{i};
Source=Sources{i};
freq=freqs{i};
if Source==1
    [ T1{1,i},T2{1,i},Fx,Fy,Fz{1,i},Tx,Ty,Tz,t{1,i} ] = ATIOLD( file,freq );

elseif Source==2
    [ T1{1,i},T2{1,i},Fz{1,i},t{1,i} ] = VACE( file );

elseif Source==3
    [ T1{1,i},T2{1,i},Fz{1,i},Fz{2,i},t{1,i} ] = CooperOLD( file,freq );
    t{2,i}=t{1,i};
    T1{2,i}=T1{1,i};
    T2{2,i}=T2{1,i};
    %Fz=Fz2;  %Select Appropriate Cooper Cell of Interest
elseif Source==4
    [ T1{1,i},T2{1,i},Fx,Fy,Fz{1,i},Tx,Ty,Tz,t{1,i} ] = ATI_Timed( file );

elseif Source==5
    [ T1{1,i},T2{1,i},Fz{1,i},Fz{2,i},t{1,i} ] = Cooper_Timed( file );
    t{2,i}=t{1,i};
    T1{2,i}=T1{1,i};
    T2{2,i}=T2{1,i};

elseif Source==6
    [ T1{1,i},T2{1,i},Fz{1,i},Fz{2,i},Fz{3,i},t{1,i} ] = Combined( file );
    t{2,i}=t{1,i};
    t{3,i}=t{1,i};
    T1{2,i}=T1{1,i};
    T2{2,i}=T2{1,i};
    T1{3,i}=T1{1,i};
    T2{3,i}=T2{1,i};

elseif Source==7
    [ T1{1,i},T2{1,i},T1{2,i},T2{2,i},Fz{1,i},Fz{2,i},t{1,i} ...
        ,t{2,i} ] = VACE1( file );

else
   display('ERROR: Bad Source Selected');
end
i=i+1;
```

```
end

end
```

```
function [ T1,T2,Fz,t ] = crop( T1,T2,Fz,t )
%This function crops the loadup and unload portions of the data
%and filters any bad data points, accepts variables in cell form
%   Created by Justin Heppe
%   Last update: 17 Feb 2015

%%
[m,n]=size(Fz);
j=1;

while j <= m
    i=1;
    while i<=n
    %Pull out the arrays desired
    T11=T1{j,i};
    T21=T2{j,i};
    Fz1=Fz{j,i};
    t1=t{j,i};
    p=size(Fz1);
    if p(2)<=20
        i=i+1;
    else
        %First remove low values (<.01)
        l1=find(Fz1<.01);
        Fz1(l1)=[];
        t1(l1)=[];
        T11(l1)=[];
        T21(l1)=[];

        %Now remove those points too far off from the path
        Fzlog=log(Fz1);
        tlog=log(t1);
        [f1,gof]=fit(tlog',Fzlog','poly2');
        F1=f1(tlog);
        diff=F1'-Fzlog;
        d=abs(diff);
        l2=find(d>0.1);
        Fz1(l2)=[];
        t1(l2)=[];
        T11(l2)=[];
        T21(l2)=[];

        %Now find the highest value and begin from there
        [q,l3]=max(Fz1);
        Fz1(1:l3)=[];
        t1(1:l3)=[];
        T11(1:l3)=[];
        T21(1:l3)=[];

        %Now adjust all the times to begin at zero
        t1=t1-t1(1);
```

```
        %Crop time if necessary
         l3=find(t1>100000);
%         Fz1(l3)=[];
%         t1(l3)=[];
%         T11(l3)=[];
%         T21(l3)=[];

        %Normalize Relaxation by Percentage of Initial Value
        %Can be used to normalize at a chosen point in time
        Fz1=Fz1./mean(Fz1(l3(1):l3(10)));

        %Return values to the cells
        T1{j,i}=T11;
        T2{j,i}=T21;
        Fz{j,i}=Fz1;
        t{j,i}=t1;
        i=i+1;
    end
    end
    j=j+1;
end

end
```

```
function [ Fz ] = Temperature( T1,T2,Fz,t,Source )
%Modifies load to compensate for temperature
%   Created by Justin Heppe
%   Last update: 17 Feb 2015

%%
[m,n]=size(Fz);

for j=1:m
    i=1;
while i<=n
    %Pull out the arrays desired
    T11=T1{j,i};
    T21=T2{j,i};
    Fz1=Fz{j,i};
    t1=t{j,i};
    Source1=Source{1,i};

    if size(T11)<30
        i=i+1;
    else
    %Adjust for Temperature
    if Source1 == 1
        slope=5.6; %Correction Factor

    elseif Source1 == 2
        slope=-.21;

    elseif Source1 == 3
        slope=0;

    elseif Source1 == 4
        slope=5.6;

    elseif Source1 == 5
        slope=0;

    elseif Source1 == 6
        if j<=2;
            slope=0;
        else
            slope=5.6;
            j
        end

    elseif Source1 == 7
        slope=-.21;

    else
            display('Error: Invalid Source Selection')
    end
```

```
T=T11;

TC=mean(T(1:20));

Fz1=Fz1-slope.*(T-TC);

    %Return values to the cells
    Fz{j,i}=Fz1;

    i=i+1;
    end
end
    j=j+1;
end

end
```

```
function [ t,Fz,T1,T2 ] = reducer( t,Fz,T1,T2,N )
%Function takes in cell of force points (Fz) and
%temperature points (T11) over a time (t)and
%reduces the number of points to N
%   Created by Justin Heppe
%   Last update: 17 Feb 2015

%%
[m,n]=size(Fz);

for j=1:m
   for k=1:n
    %Pull out the arrays desired
    T11=T1{j,k};
    T21=T2{j,k};
    Fz1=Fz{j,k};
    t1=t{j,k};
    p=size(Fz1);

    %Begin Reducer
    s=size(Fz1);
    s=s(2);

    %Reduce points to a preset number by averaging
    l=1;
    i=1;
    d=s/N;       %number of points in each average
    d=fix(d);     %make integer
    TR1=[];
    TR2=[];
    FR=[];
    tR=[];


        while i<=s-d-1  %Loop for averaging L-1 points
            SectionForce=Fz1(i:i+d);
            SectionTime=t1(i:i+d);
            SectionTemp1=T11(i:i+d);
            SectionTemp2=T21(i:i+d);
            PointForce=mean(SectionForce);
            FR(l)=PointForce;
            PointTime=median(SectionTime);
            tR(l)=PointTime;
            PointTemp1=mean(SectionTemp1);
            TR1(l)=PointTemp1;
            PointTemp2=mean(SectionTemp2);
            TR2(l)=PointTemp2;
            l=l+1;
            i=i+d+1;
        end

   T1{j,k}=TR1;
```

```
    T2{j,k}=TR2;
    Fz{j,k}=FR;
    t{j,k}=tR;
    end

end
end
```

```
function [ Fz,t ] = redistribute( Fz,t )
%Pushes the weighting of points to the earlier region of the data
%by adjusting the time points to a log scale and interpolating the
%points
%   Created by Justin Heppe
%   Last update: 17 Feb 2015

%%
[m,n]=size(Fz);

j=1;
if j<=m
    i=1;
while i<=n
    Fz1=Fz{j,i};
    t1=t{j,i};
    if numel(t1)==0
        i=i+1;
    else
    tRLog=t1;
    tRLog(2:end)=logspace(log10(t1(2)),log10(t1(end)),length(t1)-1);
    FzRLog=interp1(t1,Fz1,tRLog,'pchip','extrap');

    Fz{j,i}=FzRLog;
    t{j,i}=tRLog;
    i=i+1;
    end
end
j=j+1;
end
end
```

```
function [ a, b, ci ] = StressFittingUnknown( t, Fz )
%Function to perform curve fitting of stress relaxation data based on ?
%   Outputs in the following form:
%   FzR= a1 - a2*(1-exp(-tR*b1) - a3*(1-exp(-tR*b2*b1)
%   Inputs are time (tR), force (FzR)
%   Created by Justin Heppe
%   Last update: 17 Feb 2015

%%
[m,n]=size(Fz);

j=1;
while j<=m
    i=1;
while i<=n
    Fz1=Fz{j,i};
    t1=t{j,i};
    if numel(t1)==0
        i=i+1;
    else
        %Input equation to fit to
        ft=fittype('a0-a1*(1-exp(-x*b1/100000))-a2*(1-exp(-x*b1*b2/100000))');

        %Set bounds and other fitting options
        options=fitoptions(ft);
        options.Lower=[0 0 0 0 0];
        options.Upper=[15 2 20 200 0.2];
        options.Start=[10 0.5 0.5 5e-5 5e-7];
        options.Robust='Bisquare';

        %Perform the Fit
        [f1,gof]=fit(t1',Fz1',ft,options);

        %Create a set of data using the fit equation
        s=size(t1);
        s2=s(2);
        FzF=f1(t1);

        %Plot the fit results
        figure(1501)
        hold on
        %Plot data
        plot(t1,Fz1)
        %Plot fit
        plot(f1)
        xlabel('Time (s)'); ylabel('Force (N)');
        title('Stress Relaxation Fit');

        %Create variables with fit values
        coeffvals=coeffvalues(f1)
        gof
        c(1)=coeffvals(1);
```

```
        c(2)=coeffvals(2);
        c(3)=coeffvals(3);
        d(1)=coeffvals(4);
        d(2)=coeffvals(5);
        ci{j,i} = confint(f1);
        a{j,i}=c;
        b{j,i}=d;

        %Plot vertical lines designating 98% points of exponential terms
        plot(100000/coeffvals(4)*2.2*[1,1],f1(100000/coeffvals(4)...
            *2.2)*[0.9,1.1],'g-')
        plot(100000/coeffvals(4)/coeffvals(5)*2.2*[1,1],...
            f1(100000/coeffvals(4)/coeffvals(5)*2.2)*[0.9,1.1],'g-')

        %Plot each segment of fit equation
        plot(c(1));
        plot(t1,c(1)-c(2)*(1-exp(-t1.*d(1)/100000)))
        plot(t1,c(1)-c(3)*(1-exp(-t1.*d(1)*d(2)/100000)))

        %Plot fitting values
        figure(1502)
        hold on
        plot(1,c(1),'x',2,c(2),'x',3,c(3),'x',4,d(1),'o',5,d(2),'o')
        title('Fitting Value')

        i=i+1;
    end
end
j=j+1;
end

end
```

```
function [ a, b ] = StressFittingForced( t, Fz )
%Function to perform curve fitting of stress relaxation data based on ?
%   Outputs in the following form:
%   FzR= a1 - a2*(1-exp(-tR*b1) - a3*(1-exp(-tR*b2*b1)
%   Inputs are time (tR), force (FzR)
%   Created by Justin Heppe
%   Last update: 17 Feb 2015

%%
[m,n]=size(Fz);

j=1;
while j<=m
    i=1;
while i<=n
    %Pull out data to manipulate
    Fz1=Fz{j,i};
    t1=t{j,i};

    %If data set is empty move on to next
    if numel(t1)==0
        i=i+1;
    else
        %Input fitting equation
        ft=fittype('a0-a1*(1-exp(-x*20/100000))-a2*(1-exp(-x*0.3/100000))');

        %Input fitting options
        options=fitoptions(ft);
        options.Lower=[0 0 0];
        options.Upper=[15 2 2];
        options.Start=[10 0.5 0.5];
        options.Robust='Bisquare';

        %Perform fit
        [f1,gof]=fit(t1',Fz1',ft,options);

        %Plot fitting
        figure(1501)
        hold on
        %Plot data
        plot(t1,Fz1)
        %Plot fit line
        plot(f1,'g')
        xlabel('Time (s)'); ylabel('Force (N)');
        title('Stress Relaxation Fit');

        %Pull out fitting values
        coeffvals=coeffvalues(f1)
        gof
        c(1)=coeffvals(1);
        c(2)=coeffvals(2);
        c(3)=coeffvals(3);
```

```
        a{j,i}=c;

        i=i+1;
    end
end
j=j+1;
end

end
```

Appendix B

```
%   SHAPEANALYSIS.m
%Imports and Plots Shape Analysis for the cross section data
% Created by Justin Heppe
% Last update 17 Feb 2015

%%
%List the file desired to analyze
fileID=fopen('./SurfaceData/Test_1thru6_All_4Focus_ToptoMidFront.txt');

formatSpec= '%f %f %f';

%Data files and values determined
%./SurfaceData/Test_4and2_2_ToptoMidFront.txt
%j=57, i=9, f1<-100, f2>-422, f3<20
%Test_4and2_4_ToptoMidFront
%j=60, i=9 f1<-100, f2>-434, f3>40
%Test_1thru6_All_4Focus_ToptoMidFront
%j=56, i=15 For 4: F1<-100, F2>-447, F3>-25, F4<-75

%%
% Input values for number of cross sections (l1)
% and number of scans performed (l2)
l1=56;
l2=15;

for j=1:l1
for i=1:l2

    %Open file
    R{j,i}=textscan(fileID, formatSpec, 'HeaderLines',1,'Delimiter','/t');

    %Split data from cell to array
    Q=[R{j,i}(1) R{j,i}(2) R{j,i}(3)];

    %Clean the cross sections of unncessary data
     F1=find(Q{2}<-100);
     F2=find(Q{3}>-447);
     F3=find(Q{1}>-25);
     F4=find(Q{1}<-75);
     F=cat(1,F1,F2,F3,F4);
     Q{1}(F)=[];
     Q{2}(F)=[];
     Q{3}(F)=[];

     %Plot cross section data (use to determine unnessary data areas)
     hold on
     scatter3(Q{1},Q{2},Q{3})
     xlabel('x');ylabel('y');zlabel('z')
```

```
        %Flatten data from 3D to 2D
        XYZ=cell2mat(Q);
        [a,XY0{j,i}]=princomp(XYZ);

        %Plot each cross section
        figure(j)
        hold on
        scatter(XY0{j,i}(:,1),XY0{j,i}(:,2))
        xlabel('x');ylabel('y');
        daspect([1 1 1])
        hold off
    end
    end
```

```
%   SHAPEANALYSIS_2.m
% Fits data created by SHAPEANALYSIS.m
% Created by Justin Heppe
% Last update 17 Feb 2015
%Must first run SHAPEANALYSIS.m
%B results are as follows:
%B=[ry rx . .] the x0 and y0 values are incorrect

%%
for j=1:l1
for i=1:l2

    %Pull out cross section data for fitting
    XY=[XY0{j,i}(:,1) XY0{j,i}(:,2)];
    A{j,i} = EllipseFitByTaubin(XY);

    %Determine Implicit equation values from general equation values
    B{j,i} = GeneraltoImplicitEllipse( A{j,i},XY );
end
end

%%
% 1 thru 6 _4 fit only logical progress from 41 to 1
% 2 and 4 _4 fit only logical progress from 13-60

%%
%Create the time variable
x=[0; 10; 20; 30; 45; 60; 90; 120; 186; 306; 490; 1406; 2826; 8618; 10048];
%x=(1:9)';
%x=[0 60 120 240 1140 4020 5400 6900 16860]';
%set j

%%
% Calculate and plot the slope of the change in minor axis or major axis
% radii over time
for j=1:41
    for i=1:l2
        %Pull out the minor axis and major axis radii data
        rx(i)=B{j,i}(2); %minor axis
        ry(i)=B{j,i}(1); %major axis
    end

    %Fit the minor axis and major axis radii data
    f1{j}=fit(x,rx','poly1');
    coeffvalx{j}=coeffvalues(f1{j});
    f2{j}=fit(x,ry','poly1');
    coeffvaly{j}=coeffvalues(f2{j});

    %Plot the radii values
    figure(1)
    hold on
    plot(x,ry')
```

```
    xlabel('Time (s)')
    ylabel('Radius (mm)')
    hold off

    %Plot the slope values
    figure(2)
    hold on
    %plot(j,coeffvalx{j}(1),'x')
    plot(j,coeffvaly{j}(1),'o')
    xlabel('Cross Section Data Point')
    ylabel('Slope of Major Axis Radius over Time')
    hold off
end
```

```
function [ B ] = GeneraltoImplicitEllipse( A,XY )
%Takes general ellipse equation and returns implicit ellipse equation
% See   Jennings, A., Black, J., and Gutierrez,A.
%       "Geometry and Moments of Bent Tape Springs"
%       54th AIAA/ASME/ASCE/AHS/ASC Structures,
%       Structural Dynamics and Materials Conference(2013).
% For details on the equations used
% Created by Justin Heppe
% Last update 17 Feb 2015

%%
%Call out each value
a=A(1);
b=A(2);
c=A(3);
d=A(4);
f=A(5);
g=A(6);

%Calculate rotation of ellipse
theta=atan(b*2/(c-a))/2;

%Remove the rotation from each value
a1=a*cos(theta)^2+b*cos(theta)*sin(theta)+c*sin(theta)^2;
%b1=0;
c1=a*sin(theta)^2-b*cos(theta)*sin(theta)+c*cos(theta)^2;
d1=d*cos(theta)+f*sin(theta);
e1=-d*sin(theta)+f*cos(theta);
f1=g;
x1=-d1/2*a1;
y1=-e1/2*c1;

%Calculate the major and minor axis radii
a=sqrt((-4*f1*a1*c1+c1*d1^2+a1*e1^2)/(4*a1*c1^2));
b=sqrt((-4*f1*a1*c1+c1*d1^2+a1*e1^2)/(4*a1^2*c1));

%These equations are incorrect but not necessary
x0=x1*cos(theta)-y1*sin(theta);
y0=x1*sin(theta)-y1*cos(theta);

B=[a b x0 y0];


end
```

REPORT DOCUMENTATION PAGE

Form Approved
OMB No. 0704–0188

1. REPORT DATE *(DD–MM–YYYY)*	2. REPORT TYPE	3. DATES COVERED *(From — To)*
26–03–2015	Master's Thesis	Sept 2013 — Mar 2015

4. TITLE AND SUBTITLE

Methods of Measuring Stress Relaxation in Composite Tape Springs

5a. CONTRACT NUMBER

5b. GRANT NUMBER

5c. PROGRAM ELEMENT NUMBER

6. AUTHOR(S)

Heppe, Justin T., Captain, USAF

5d. PROJECT NUMBER

5e. TASK NUMBER

5f. WORK UNIT NUMBER

7. PERFORMING ORGANIZATION NAME(S) AND ADDRESS(ES)

Air Force Institute of Technology
Graduate School of Engineering and Management (AFIT/EN)
2950 Hobson Way
WPAFB OH 45433-7765

8. PERFORMING ORGANIZATION REPORT NUMBER

AFIT-ENY-MS-15-M-221

9. SPONSORING / MONITORING AGENCY NAME(S) AND ADDRESS(ES)

Air Force Research Laboratory, Space Vehicles Directorate
Mr. Whitney Reynolds
3550 Aberdeen Ave SE, Bldg. 472
Kirtland AFB, 87117
whitney.reynolds.1@us.af.mil

10. SPONSOR/MONITOR'S ACRONYM(S)

AFRL/RVSVS

11. SPONSOR/MONITOR'S REPORT NUMBER(S)

12. DISTRIBUTION / AVAILABILITY STATEMENT

Distribution Statement A: Approved for Public Release; Distribution Unlimited.

13. SUPPLEMENTARY NOTES

14. ABSTRACT

Composite tape springs present an opportunity to use stored energy for the deployment of space structures. Concern has risen over the dissipation of strain energy during storage due to viscoelasticity inherent in polymeric materials commonly used as the composite matrix. Tests to measure the internal behavior of a composite tape spring over time are conducted along with methods of analyzing and fitting the resulting data. The three constant strain configurations tested were compression force of the cross section, a restraining force of a longitudinal fold, and the change in shape of a folded section. While the shape changing test did not appear to be sensitive enough, the stress tests proved useful for measuring relaxation.

15. SUBJECT TERMS

Tape Spring, Stress Relaxation, Viscoelasticity, Physical Aging

16. SECURITY CLASSIFICATION OF:			17. LIMITATION OF ABSTRACT	18. NUMBER OF PAGES	19a. NAME OF RESPONSIBLE PERSON
a. REPORT	b. ABSTRACT	c. THIS PAGE			Dr. Alan Jennings, AFIT/ENY
U	U	U	U	104	19b. TELEPHONE NUMBER *(include area code)* (937) 255-3636, x7495; alan.jennings@afit.edu